DIFFUSION IN ALUMINUM ALLOYS

BY

ACTIVATION ANALYSIS

A STUDY OF DIFFUSION IN ALUMINUM-RICH ALLOYS OF ALUMINUM, ZINC, AND COPPER BY ACTIVATION ANALYSIS

By

ZIA-UL-HAQ

A Thesis

Submitted to the Faculty of Graduate Studies

in Partial Fulfilment of the Requirements

for the Degree

Master of Engineering

McMaster University

September 1962

MASTER OF ENGINEERING (1962) McMASTER UNIVERSITY
(Metallurgy) Hamilton Ontario

TITLE: A Study of Diffusion in Aluminum-rich Alloys of Aluminum, Zinc and Copper by Activation Analysis

AUTHOR: Zia-ul-Haq, B.Sc. Eng (Dacca University, Pakistan)

SUPERVISOR: Professor J. S. Kirkaldy

NUMBER OF PAGES: v, 36

SCOPE AND CONTENTS:

In this thesis, a theoretical study of certain properties of the diffusion coefficient matrix in a multicomponent system has been carried out. The ratio of the off-diagonal diffusion coefficient to the on-diagonal diffusion coefficient in a dilute ternary substitutional system has been evaluated theoretically. The effect of the second solute gradient on the diffusivity of the first one in a ternary substitutional solid solution has been experimentally determined using the neutron activation analysis technique.

ACKNOWLEDGMENTS

The author wishes to express his appreciation to Dr. J. S. Kirkaldy for the constant interest and guidance which he offered during the course of this work. The staff of the McMaster Reactor (in particular Drs. W. H. Fleming and R. H. Tomlinson) and the technical staff of the Department of Metallurgy and Metallurgical Engineering (H. Neumayer) provided invaluable assistance with the experiments. The author is grateful for a Colombo Plan scholarship and for the financial support of the National Research Council of Canada in the form of grant-in-aid (A 697) to Dr. Kirkaldy. Thanks are due to the staff and the graduate students (G. Purdy) for frequent stimulating discussions.

TABLE OF CONTENTS

INTRODUCTION

It is well known that many physical processes such as chemical diffusion, heat conduction and elastoplastic behaviour of solids can be usefully approximated by linear (sometimes generalized linear as in the case of elastic properties) phenomenological relations. Fick's law for chemical diffusion is a particular case. This introduces the diffusion rate constant or diffusion coefficient as a measure of the material transport of one component into another under specific conditions (generally isothermal and isobaric).

The conventional technique for determining the rate-constant is to weld two pieces of metals together as a 'couple', to anneal the 'couple' at a constant predetermined temperature for a reasonable period and to analyse compositions at different distances from the weld interface on either side. From the knowledge of chemical analysis as a function of distance, time and temperature one can calculate the diffusion coefficient.

The binary diffusional analysis is straightforward (see page 4). However, to deal with multicomponent systems one has to assume extended linear relations and to account for both on-diagonal and off-diagonal terms in the diffusion coefficient matrix. To justify the assumption of generalized phenomenological relations in handling multicomponent diffusion one has to invoke the principles of irreversible thermodynamics. We will have occasions to

discuss these later in detail.

In this paper a theoretical investigation of certain properties of the matrix of the multicomponent diffusion coefficients has been carried out. In addition the diffusion coefficients for the ternary system Aℓ-Zn-Cu have been obtained from experimental measurements using the activation analysis technique. The advantage and the scope of this method of analysis has also been elaborated.

The thermodynamic theory of multicomponent concentration-dependent diffusion due to Onsager[15] has been exploited by Gosting[8] and co-workers in liquid electrolytes and by Darken[4] and Kirkaldy[11] in alloy systems. The mathematical theory for the diffusion couple is an extension of the analysis of Boltzmann[2] and Matano[14] for a binary system.

The experimental study presented here follows rather closely that used by Mason[13] for the system Aℓ-Cu-Mn. Activation analysis of the semi-infinite diffusion couples in the system Aℓ-Zn-Cu has produced an experimental specification of the diffusion constant for this system. The accuracy of the activation method is particularly suited to the small samples available for analysis.

THEORY

The process of diffusion is an irreversible phenomenon. The 'force' and the response to this force are the two basic aspects of interest to an investigator. The following thermodynamic formulation of an irreversible process is due to Callen[3]. If in a composite system consisting of several subsystems certain extensive parameters are conserved, and assuming a functional dependence of the local entropy on the extensive parameters in an infinitesimal region and the freedom of the extensive variable within any subsystem, the vanishing of the partial derivatives with respect to the extensive parameter determines the equilibrium of the system. Mathematically this means

$$(1) \qquad A_k \equiv \left(\frac{\partial S}{\partial X_k}^{eq}\right)_{X_k^{eq}} = 0 \quad \text{(at equilibrium)}$$

where A_k is the 'affinity' corresponding to the k'th subsystem and X_k is the extensive parameter.

Since each local flux J_k depends only upon instantaneous local affinities and upon the local intensive parameter and because each flux is known to vanish as the affinities disappear (since by definition $J_k \equiv \frac{dX_k}{dt}$), J_k can be expanded in powers of the affinities.

$$(2) \qquad J_k = \sum_j \frac{\partial J_k}{\partial A_j} A_j + \frac{1}{2!} \sum_{i,j} \frac{\partial^2 J_k}{\partial A_i} \frac{}{\partial A_j} A_i A_j + \cdots$$

Ignoring the derivatives of higher order a linear relation between

the affinities and the flux is obtained.

$$(3) \qquad J_k = \sum_j \frac{\partial J_k}{\partial A_j} A_j$$

This formulation lays the groundwork for a systematic analysis of diffusion. It may be noticed that the vanishing of the affinities at equilibrium is an alternate statement of entropy maxima.

Starting from an experimental point of view, Adolf Fick[6] in 1855 formulated his first law of diffusion of a single component in a binary solution

$$(4) \qquad J = - D \frac{\partial C}{\partial x}$$

where J is the diffusion current in concentration units per unit area per unit time, D is the diffusion coefficient in units of area per unit time, C is the concentration (say in moles per unit volume) and x is the distance.

The second law immediately follows from the continuity condition, which is

$$(5) \qquad \text{div } J + \frac{\partial C}{\partial t} = 0$$

giving

$$(6) \qquad \frac{\partial C}{\partial t} = \frac{\partial}{\partial x} \left(D \frac{\partial C}{\partial x} \right),$$

or for constant D,

$$(7) \qquad \frac{\partial C}{\partial t} = D \frac{\partial^2 C}{\partial x^2} .$$

In a semi-infinite diffusion couple, the initial

conditions are

(8) $C = C^o$ for $x > 0$ and $t = 0$

$C = C'$ for $x < 0$ and $t = 0$

and the corresponding solution[1] to equation (7) is

$$(9) \qquad C = C^o + \frac{1}{2}\,(C' - C^o)\left(1 - \operatorname{erf}\,\frac{x}{2\sqrt{Dt}}\right)$$

Values for the error function can be obtained from a standard table[17] of functions.

In the more general case where D is concentration dependent an iterable solution[2] for the general equation (6) is

$$(10) \qquad C = C^o + (C' - C^o)\,\frac{\int_{\lambda}^{\infty} \frac{d\lambda'}{D(\lambda)}\, e^{-\int_o^{\lambda'} \frac{\lambda'' d\lambda''}{2D(\lambda'')}}}{\int_{-\infty}^{\infty} \frac{d\lambda'}{D(\lambda')}\, e^{-\int_o^{\lambda'} \frac{\lambda'' d\lambda''}{2D(\lambda'')}}} \quad ; \quad \lambda = \frac{x}{\sqrt{t}}$$

If D is constant its value can be found from experiment by fitting (9) to the experimental results. However, for a concentration dependent diffusion coefficient the Boltzmann-Matano analysis must be used as described in the following. Boltzmann[2], in 1894, was able to reduce the partial differential equation (6) to an ordinary one by introducing a single variable $\lambda = \frac{x}{\sqrt{t}}$. On substitution, equation (6) assumes the form

$$(11) \qquad -\frac{1}{2}\,\lambda\,\frac{dC}{d\lambda} = \frac{d}{d\lambda}\left(D\,\frac{dC}{d\lambda}\right) .$$

Multiplying throughout by $d\lambda$ and transposing,

$$(12) \qquad d\left(D\,\frac{dC}{d\lambda}\right) = -\frac{1}{2}\,\lambda\,dC$$

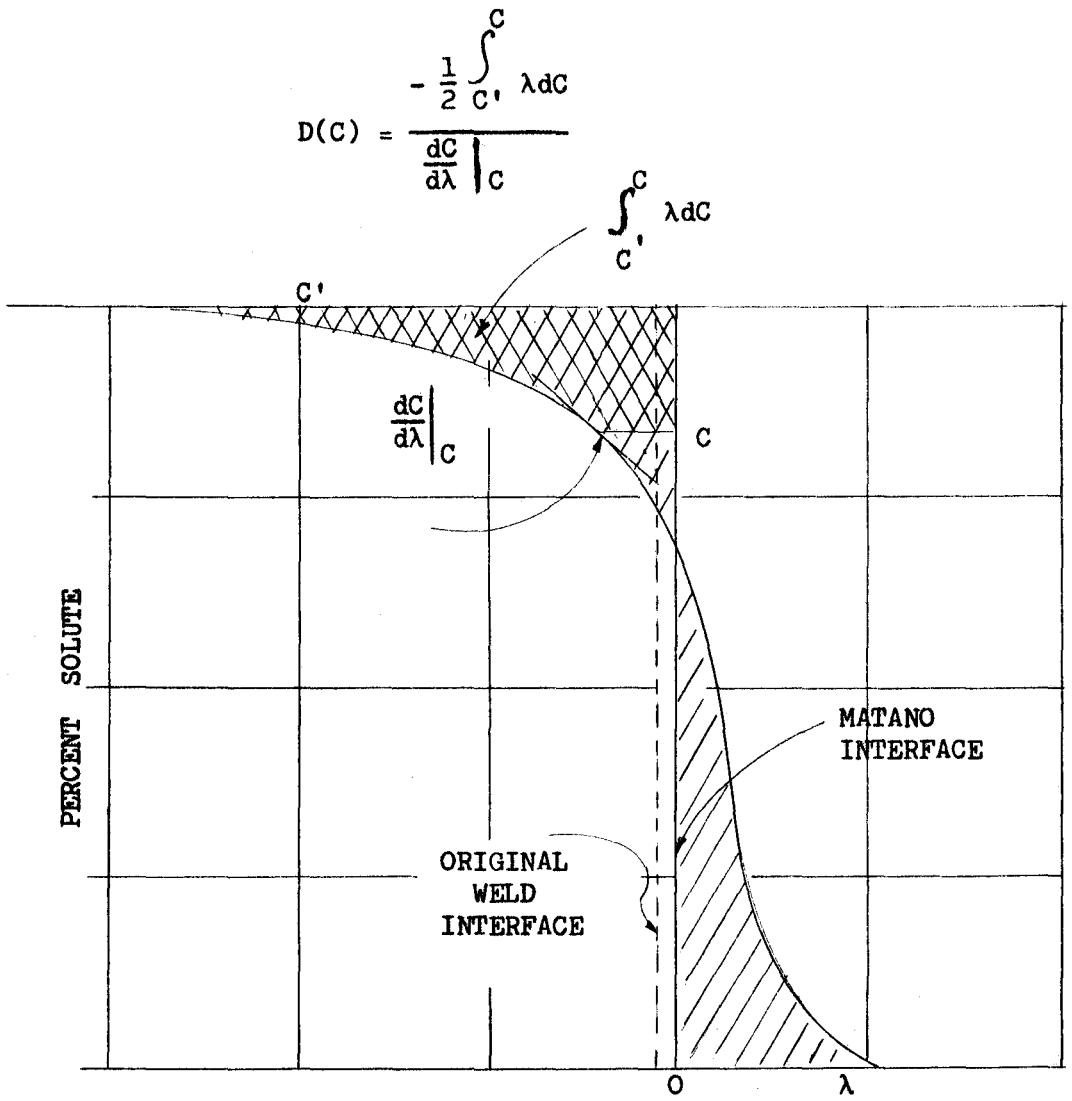

Figure 1. Typical penetration curve for concentration-dependent diffusion in a binary system.

Integrating from $C = C'$ (where $\frac{dC}{d\lambda} = 0$) to C,

$$(13) \qquad D \frac{dC}{d\lambda} = -\frac{1}{2} \int_{C'}^{C} \lambda dC$$

or

$$(14) \qquad D(C) = \frac{-\frac{1}{2} \int_{C'}^{C} \lambda dC}{\left.\frac{dC}{d\lambda}\right|_{C}}$$

This relation given by Boltzmann, later empirically derived by Matano[14], is generally used in evaluating D from an experimental diffusion penetration curve, such as shown schematically in figure 1. The distance origin or "Matano interface" is to be so chosen such that the two shaded areas are equal. This corrects for the movement of the original weld interface, (if there be any), due to the Kirkendall effect. In the case of ternary systems and multicomponent systems of higher order the presence of concentration gradients of other constituents introduces complications.

Onsager[15] generalized Fick's diffusion equation for an n-component system as a linear expression in all the concentration gradients.

$$(15) \qquad J_i = -\sum_{k=1}^{n} D'_{ik} \nabla C_k, \quad (i = 1,2,\cdots n)$$

However, the alternative description utilizing chemical potential gradients (isothermal) or partial molal free energy gradients as the generalized forces for diffusion due to Onsager and Fuoss[16],

$$(16) \qquad J_i = -\sum_{k=1}^{n} L_{ik} \nabla \mu_k, \quad (i = 1,2,\cdots n),$$

is more fundamental, if less practicable. Important works on the transformation relation between (15) and (16) have been worked out by Hooyman[9] basically following a suggestion made by Onsager[15]. Some aspects of these transformations as applied to diffusion in substitutional alloys have been clarified by Kirkaldy[11]. If the units of concentration are so chosen that (here moles per unit volume or atoms per unit volume),

$$(17) \qquad \sum_{i=1}^{n} C_i = \text{constant}$$

then equation (15) can be written as

$$(18) \qquad J_i = - \sum_{k=1}^{n-1} D_{ik} \nabla C_k, \quad D_{ik} = D'_{ik} - D'_{in}$$

Since in a substiutional alloy the lattice sites are conserved

$$(19) \qquad \sum_{i=1}^{n} J_i = 0$$

The D_{ik} in equation (18) satisfy the relations

$$(20) \qquad \sum_{i=1}^{n} D_{ik} = 0$$

and the continuity condition for the i,th component is

$$(21) \qquad \nabla . J_i + \frac{\partial C_i}{\partial t} = 0$$

Combining (18) and (21) the generalized diffusion equation becomes

$$(22) \qquad \frac{\partial C_i}{\partial t} = \sum_{k=1}^{n-1} \nabla . (D_{ik} \nabla C_k)$$

De Groot[5] has shown that, in equation (16)

$$(23) \qquad \sum_{k=1}^{n} L_{ik} = 0$$

$$(24) \qquad \sum_{i=1}^{n} L_{ik} = 0$$

The principle of 'microscopic reversibility' demands that $[L_{ik}]$ should be symmetric, that is,

$$(25) \qquad L_{ik} = L_{ki} \ .$$

Rewriting equation (16)

$$J_k = - \sum_{j=1}^{n} L_{kj} \nabla \mu_j$$

$$= - \sum_{j=1}^{n} L_{kj} \sum_{i=1}^{n-1} \mu_{ji} \nabla C_i$$

$$= - \sum_{i=1}^{n-1} D_{ki} \nabla C_i$$

where $\mu_{ik} = \dfrac{\partial \mu_i}{\partial C_k}$, gives

$$(26) \qquad D_{ki} = \sum_{j=1}^{n} L_{kj} \mu_{ji}, \ (i,k = 1,2, \cdots n-1)$$

Using the relations (23) and the modified Gibbs-Duhem relation

$$(27) \qquad \mu_{ni} = - \sum_{\ell=1}^{n-1} \frac{C_\ell}{C_n} \mu_{\ell i} \ , \ (i = 1, 2, \cdots n-1)$$

in the equation (26) we obtain

$$(28a) \qquad D_{ki} = \sum_{p,\ell=1}^{n-1} L_{kp} \left(\frac{C_\ell}{C_n} + \delta_{p\ell} \right) \mu_{\ell i}, \ \delta_{p\ell} \text{ being}$$

the kronecker delta and $(i = 1,2, \cdots n-1)$

In matrix notation* this would read

$$(28b) \qquad \left[D_{ki} \right] = \left[L_{kp} \right] \left[\frac{C_\ell}{C_n} + \delta_{p\ell} \right] \left[\mu_{\ell i} \right] \ ,$$

all the matrices being square of (n-1) degree.

---

* The subscript for row besides $\dfrac{C_\ell}{C_n}$ being superfluous, has been omitted.

$\left[L_{kp}\right]$ is symmetric with all on-diagonal terms positive. Consequently $\left|L_{kp}\right| > 0$, as are all the principal minors. $\left[\frac{\partial \mu}{\partial C}\right]$ is to be studied further.

Now

$$(29) \qquad \mu_i = \mu_i (C_1, C_2 \cdots C_{n-1})$$

where $$C_k = \frac{N_k}{\sum_{p=1}^{n} N_p} = \frac{N_k}{K}, \quad K = \sum_{p=1}^{n} N_p$$

and the N's are the mole number for each component in the system.

Thus

$$(30) \qquad \frac{\partial \mu_i}{\partial N_k} = \sum_{j=1}^{n-1} \frac{\partial \mu_i}{\partial C_j} \frac{\partial C_j}{\partial N_k}$$

But as a result of the relation

$$\frac{\partial C_j}{\partial N_k} = \left(\frac{\delta_{jk}}{K} - \frac{N_j}{K^2}\right),$$

the equation (30) becomes

$$(31a) \qquad \frac{\partial \mu_i}{\partial N_k} = \sum_{j=1}^{n-1} \frac{\partial \mu_i}{\partial C_j} \left(\frac{\delta_{jk}}{K} - \frac{N_j}{K^2}\right) = \sum_{j=1}^{n-1} \mu_{ij} \left(\frac{\delta_{jk}}{K} - \frac{N_j}{K^2}\right)$$

or in matrix notation*

$$(31b) \qquad \left[\frac{\partial \mu_i}{\partial N_k}\right] = \frac{1}{K^2} \left[\mu_{ij}\right] \left[K\delta_{jk} - N_j\right]$$

From Maxwell's relations[18], $\left[\frac{\partial \mu_i}{\partial N_k}\right]$ is symmetric and for stable solutions has all positive diagonal terms. The diffusion coefficient matrix in (28b) now reads using relation (31b)

---

* The subscript for column besides N_j, being superfluous has been omitted.

$$(32) \qquad [D] = [L]\left[\frac{C_\ell}{C_n} + \delta_{p\ell}\right] K^2 \left[\frac{\partial \mu}{\partial N}\right] \left[K\delta_{jk} - N_j\right]^{-1},$$

where for the sake of conciseness the subscripts in the matrices $[D]$, $[L]$ and $\left[\frac{\partial \mu}{\partial N}\right]$ have been omitted.

All the matrices in (32) are square and are of the same order (n-1). Hence the product of the determinants of all the matrices on the right hand side is equal to the determinant of the product matrix.

$$(33a) \qquad |D| = |L| \left|\frac{C_\ell}{C_n} + \delta_{p\ell}\right| (K^2)^{n-1} \left|\frac{\partial \mu}{\partial N}\right| \left|K\delta_{jk} - N_j\right|^{-1}$$

or

$$(33b) \qquad |D| = \left(K^{n-1}\right)^2 |L| \left|\frac{N_\ell}{N_n} + \delta_{p\ell}\right| \left|\frac{\partial \mu}{\partial N}\right| \left|K\delta_{jk} - N_j\right|^{-1}$$

In the product above,

$$(34) \qquad \left|\frac{N_\ell}{N_n} + \delta_{p\ell}\right| = \frac{K}{N_n} > 0$$

and for every solution in which N_n represents the richest component

$$(35) \qquad \left|K\delta_{jk} - N_j\right| = \prod_{i=1}^{n-1} \left(K - 2N_i\right)\left\{1 + \sum_{j=1}^{n-1} \frac{N_j}{K-2N_j}\right\} > 0$$

Keeping in mind that for a stable solution $|L| > 0$, $\left|\frac{\partial \mu}{\partial N}\right| > 0$, we have, for an n-component system subject to the inequalities (34), (35), that the diffusion coefficient determinant is always greater than zero.

$$(36) \qquad |D| > 0.$$

This general result was originally proved for n=3 by Kirkaldy[11]. While it has not been found possible to make any

general statement about the other principal minors of [D], we gain further understanding of its character by examining the individual on-diagonal terms in dilute three-component system. In this case

$$(37)\quad [D] = \begin{bmatrix} L_{11} & L_{12} \\ L_{12} & L_{22} \end{bmatrix} \begin{bmatrix} \left(1 + \frac{N_1}{N_3}\right) & \frac{N_2}{N_3} \\ \frac{N_1}{N_3} & \left(1 + \frac{N_2}{N_3}\right) \end{bmatrix} K^2 \begin{bmatrix} \frac{\partial \mu_1}{\partial N_1} & \frac{\partial \mu_1}{\partial N_2} \\ \frac{\partial \mu_1}{\partial N_2} & \frac{\partial \mu_2}{\partial N_2} \end{bmatrix} \begin{bmatrix} (N_2 + N_3) & N_1 \\ N_2 & (N_1 + N_3) \end{bmatrix}^{-1}$$

Therefore a typical diagonal element of [D] is

$$(38)\quad D_{11} = \frac{(N_1+N_2+N_3)}{N_3^2} \left[\left\{ L_{11}(N_1+N_3) + L_{12}N_1 \right\} \left\{ \frac{\partial \mu_1}{\partial N_1}(N_1+N_3) - \frac{\partial \mu_1}{\partial N_2} N_2 \right\} + \left\{ L_{11} N_2 + L_{12}(N_1+N_3) \right\} \left\{ \frac{\partial \mu_1}{\partial N_2}(N_1+N_3) - \frac{\partial \mu_2}{\partial N_2} N_2 \right\} \right]$$

For dilute solution where,

$$N_1 \ll N_3 \quad \text{and}$$
$$N_2 \ll N_3 \ ;$$

this reduces to

$$(39)\quad D_{11} \cong (N_1+N_2+N_3)\left(L_{11} \frac{\partial \mu_1}{\partial N_1} + L_{12} \frac{\partial \mu_1}{\partial N_2}\right) \cong L_{11} \frac{\partial \mu_1}{\partial X_1} + L_{12} \frac{\partial \mu_1}{\partial X_2} \ ;$$

where X's are mole fractions. At this point we can rewrite equation (16) for unidirectional diffusion in a 3-component system which for component one is

$$(40)\quad J_1 = -\left(L_{11} \frac{\partial \mu_1}{\partial x} + L_{12} \frac{\partial \mu_2}{\partial x} + L_{13} \frac{\partial \mu_3}{\partial x}\right)$$

The relation (23) and the Gibbs-Duhem equation

$$(41)\quad d\mu_3 = -\frac{N_1}{N_3} d\mu_1 - \frac{N_2}{N_3} d\mu_2$$

reduce (40) to

$$J_1 = -\left\{L_{11} + \frac{N_1}{N_3}(L_{11}+L_{12})\right\}\frac{\partial \mu_1}{\partial x} - \left\{L_{12} + \frac{N_2}{N_2}(L_{11}+L_{12})\right\}\frac{\partial \mu_2}{\partial x} \tag{42a}$$

$$\cong - L_{11}\frac{\partial \mu_1}{\partial x} - L_{12}\frac{\partial \mu_2}{\partial x} \tag{42b}$$

for dilute solution.

As $X_1 \rightarrow 0$, $J_1 \rightarrow 0$

so both L_{11} and $L_{12} \rightarrow 0$.

From the empirical relation in a dilute solution

$$\mu_1 = RT\ \ell n\ kX_1\ (1 + aX_1)(1 + cX_2) + \mu_1^o$$

where k, a, c, and μ_1^o are constants. By partial differentiation with respect to X_1 and X_2 we obtain

$$\frac{\partial \mu_1}{\partial X_1} = \frac{RT(1+2aX_1)}{X_1(1+aX_1)}$$

and

$$\frac{\partial \mu_1}{\partial X_2} = \frac{cRT}{1+cX_2}$$

respectively.

It is noticed that as $X_1 \rightarrow 0$ $\frac{\partial \mu_1}{\partial X_1} \rightarrow \infty$, while $\frac{\partial \mu_1}{\partial X_2}$ approaches a constant value. Therefore in the approximate expression for D_{11} in (39), as $X_1 \rightarrow 0$, and thereby both L_{11} and $L_{12} \rightarrow 0$, $L_{11}\frac{\partial \mu_1}{\partial X_1} \rightarrow$ finite while $L_{12}\frac{\partial \mu_1}{\partial X_2} \rightarrow 0$.

Hence D_{11} (and by symmetry D_{22}) will always be positive for stable dilute solutions of solute elements 1 and 2.

The ratio $\frac{D_{12}}{D_{11}}$ is evaluated for dilute ternary substitutional solid solution in the following analysis.

Since

$$\frac{\partial \mu_i}{\partial x} = \frac{\partial \mu_i}{\partial C_1}\frac{\partial C_1}{\partial x} + \frac{\partial \mu_i}{\partial C_2}\frac{\partial C_2}{\partial x}$$

the equation (42a) can be rewritten as

$$(43)\quad J_1 = -\left[L_{11}\left\{\left(1+\frac{N_1}{N_3}\right)\frac{\partial \mu_1}{\partial C_1} + \frac{N_2}{N_3}\frac{\partial \mu_2}{\partial C_1}\right\} + L_{12}\left\{\left(1+\frac{N_2}{N_3}\right)\frac{\partial \mu_2}{\partial C_1} + \frac{N_1}{N_3}\frac{\partial \mu_1}{\partial C_1}\right\}\right]\frac{\partial C_1}{\partial x}$$
$$-\left[L_{11}\left\{\left(1+\frac{N_1}{N_3}\right)\frac{\partial \mu_1}{\partial C_2} + \frac{N_2}{N_3}\frac{\partial \mu_2}{\partial C_2}\right\} + L_{12}\left\{\left(1+\frac{N_2}{N_3}\right)\frac{\partial \mu_2}{\partial C_2} + \frac{N_1}{N_3}\frac{\partial \mu_1}{\partial C_2}\right\}\right]\frac{\partial C_2}{\partial x}$$

Comparing (43) with the equation

$$(44)\qquad J_1 = -D_{11}\frac{\partial C_1}{\partial x} = D_{12}\frac{\partial C_2}{\partial x}$$

the ratio $\frac{D_{12}}{D_{11}}$ can be given by

$$(45)\quad \frac{D_{12}}{D_{11}} = \frac{\left(1+\frac{N_1}{N_3}\right)\frac{\partial \mu_1}{\partial C_2} + \frac{N_2}{N_3}\frac{\partial \mu_2}{\partial C_2} + \frac{L_{12}}{L_{11}}\left\{\left(1+\frac{N_2}{N_3}\right)\frac{\partial \mu_2}{\partial C_2} + \frac{N_1}{N_3}\frac{\partial \mu_1}{\partial C_2}\right\}}{\left(1+\frac{N_1}{N_3}\right)\frac{\partial \mu_1}{\partial C_1} + \frac{N_2}{N_3}\frac{\partial \mu_2}{\partial C_1} + \frac{L_{12}}{L_{11}}\left\{\left(1+\frac{N_2}{N_3}\right)\frac{\partial \mu_2}{\partial C_1} + \frac{N_1}{N_3}\frac{\partial \mu_1}{\partial C_1}\right\}}$$

$$= \frac{\left(1+\frac{X_1}{X_3}\right)\frac{\partial \mu_1}{\partial X_2} + \frac{X_2}{X_3}\frac{\partial \mu_2}{\partial X_2} + \frac{L_{12}}{L_{11}}\left\{\left(1+\frac{X_2}{X_3}\right)\frac{\partial \mu_2}{\partial X_2} + \frac{X_1}{X_3}\frac{\partial \mu_1}{\partial X_2}\right\}}{\left(1+\frac{X_1}{X_3}\right)\frac{\partial \mu_1}{\partial X_1} + \frac{X_2}{X_3}\frac{\partial \mu_2}{\partial X_1} + \frac{L_{12}}{L_{11}}\left\{\left(1+\frac{X_2}{X_3}\right)\frac{\partial \mu_2}{\partial X_1} + \frac{X_1}{X_3}\frac{\partial \mu_1}{\partial X_1}\right\}}$$

C's being moles per unit volume here.

$$(45a)\quad \simeq \frac{\left(1+\frac{X_1}{X_3}\right)\frac{\partial \mu_1}{\partial X_2} + \frac{X_2}{X_3}\frac{\partial \mu_2}{\partial X_2}}{\left(1+\frac{X_1}{X_3}\right)\frac{\partial \mu_1}{\partial X_1} + \frac{X_2}{X_3}\frac{\partial \mu_2}{\partial X_1}}$$

assuming that, the ratio $\frac{L_{12}}{L_{11}}$ is small.

Knowing that for dilute solution

$$\mu_1 = RT \ln k_1 X_1 (1 + aX_1 + cX_2) + \mu_1^o$$

$$\mu_2 = RT \ln k_2 X_2 (1 + bX_2 + cX_1) + \mu_2^o , \tag{46}$$

where k_1, k_2, a, b, c, μ_1^o and μ_2^o are constants, the required partial derivatives are

$$\frac{\partial \mu_1}{\partial X_1} = \frac{RT}{X_1} (1 + aX_1),$$

$$\frac{\partial \mu_2}{\partial X_2} = \frac{RT}{X_2} (1 + bX_2),$$

$$\frac{\partial \mu_1}{\partial X_2} = \frac{cRT}{(1 + aX_1 + cX_2)} , \tag{47}$$

and

$$\frac{\partial \mu_2}{\partial X_1} = \frac{cRT}{(1 + bX_2 + cX_1)}$$

Substituting the values from (47) in (45a) and neglecting higher powers of X_1 and X_2 we obtain the ratio

$$\frac{D_{12}}{D_{11}} \cong \frac{cX_1(1 - aX_1 - cX_2) + \frac{X_1}{X_1 + X_3}(1 + bX_2)}{(1 + aX_1) + \frac{cX_1X_2}{X_1 + X_3}(1 - bX_2 - cX_1)}$$

$$\cong cX_1(1 - aX_1)(1 - aX_1 - cX_2) + \frac{X_1}{X_1 + X_3}(1 - aX_1)(1 + bX_2)$$

$$\cong cX_1 + \frac{X_1}{X_1 + X_3}$$

$$\cong X_1 (1 + c) \tag{48}$$

If the ratio $\frac{L_{12}}{L_{11}}$ is taken into account, a better approximation for

the ratio D_{12}/D_{11}

(48a) $$\frac{D_{12}}{D_{11}} \simeq X_1(1 + c) + \frac{L_{12}}{L_{11}} \frac{X_1}{X_2} (1 - aX_1 + bX_2)$$

By calculating J_2 in the same way, we obtain the symmetrical result

(49) $$\frac{D_{21}}{D_{22}} \cong (1 + c) X_2 .$$

Combining (48) and (49),

(50) $$D_{11}D_{21} X_1 \cong D_{12}D_{22}X_2 .$$

The relation (50) has been proved for interstitial diffusion by Kirkaldy and Purdy[12] both by statistical calculations based on nearest-neighbour interactions and on chemical thermodynamic considerations. It is important to note now that the dilute solution results (48) and (49) are purely thermodynamic to the extent that the off diagonal interactions as measured by L_{12} are small.

Determination of concentration-dependent diffusion coefficients from experimental penetration curve

Considering diffusion in the x-direction we can rewrite equation (22) for an n-component system.

(22a) $$\frac{\partial C_i}{\partial t} = \sum_{k=1}^{n-1} \frac{\partial}{\partial x} \left(D_{ik} \frac{\partial C_k}{\partial x} \right)$$

In analogy to the Boltzmann-Matano analysis for binary diffusion[2] (for concentration-dependent coefficients), parametric solutions are sought of the form

(51) $$C_i = C_i(\lambda), \quad \lambda = \frac{x}{\sqrt{t}}$$

Combining (22a) and (51) the following set of non-linear ordinary differential equations is obtained

$$(52) \qquad -\frac{\lambda}{2}\frac{dC_i}{d\lambda} = \sum_{k=1}^{n-1}\frac{d}{d\lambda}\left[D_{ik}\frac{dC}{d\lambda}\right]$$

Equations (52) can be applied to a semi-infinite diffusion couple for which the initial conditions are

$$(53) \qquad C_i = C_i^o \quad \text{for } x > 0 \text{ and } t = 0 \text{ (i.e. } \lambda = \infty)$$

$$C_i = C_i' \quad \text{for } x < 0 \text{ and } t = 0 \text{ (i.e. } \lambda = -\infty)$$

From a first integration of equations (52), then,

$$(54) \qquad \frac{1}{2}\int_{C_i^o}^{C_i} \lambda dC_i = -\sum_{k=1}^{n-1} D_{ik}\frac{dC_k}{d\lambda}$$

Since one can evaluate the integral graphically and the slopes $\frac{dC_k}{d\lambda}$ from measured experimental curves, the equations (54) can be used for determining concentration-dependent diffusion coefficients. In binary alloys the procedure is the standard Boltzmann-Matano analysis and is relatively easy to work out, since only one coefficient is to be determined from a single penetration curve. For alloys of higher order the mathematics is more involved and the amount of experimental data needed is much greater. Mason[13] has investigated the experimental procedure required for a complete generalized Boltzmann-Matano analysis.

Special solution for constant diffusion coefficients in a ternary system

For the purposes of experimental analysis in this work it is sufficient to use an approximate solution for constant

coefficients which has been constructed by Kirkaldy[10] to apply to semi-infinite boundary conditions wherein

$$D_{21} \frac{d^2C_1}{d\lambda^2} << D_{22} \frac{d^2C_2}{d\lambda^2}$$

The two equations in (52) for a 3-component system are then

$$(55a) \qquad -\frac{\lambda}{2} \frac{dC_1}{d\lambda} = D_{11} \frac{d^2C_1}{d\lambda^2} + D_{12} \frac{d^2C_2}{d\lambda^2}$$

$$(55b) \qquad -\frac{\lambda}{2} \frac{dC_2}{d\lambda} = D_{22} \frac{d^2C_2}{d\lambda^2}$$

Given initial conditions (53), equation (55b) has the solution

$$(56) \qquad C_2 = C_2^o + \frac{1}{2} (C_2' - C_2^o)\left(1 - \text{erf} \frac{\lambda}{2\sqrt{D_{22}}}\right)$$

On substituting (56) in (55a), one obtains the result

$$(57) \qquad C_1 = \frac{1}{2} (C_1^o + C_1') + A \left[\text{erf} \frac{\lambda}{2\sqrt{D_{22}}} - \frac{2A - C_1^o + C_1'}{2A} \text{erf} \frac{\lambda}{2\sqrt{D_{11}}}\right]$$

where

$$A = \frac{1}{2} (C_2' - C_2^o) \frac{D_{12}}{(D_{11} - D_{22})} \quad .$$

ACTIVATION ANALYSIS

Most elements, when irradiated by the thermal neutrons of a nuclear reactor, become "activated" to form artificially radio-active species that possess individual modes of decay and radiation spectra. The rate of decay and the type of radiation emitted are characteristic of the radionuclide making it possible to identify the species uniquely in a metallic or other solution. Since the activity of a sample depends on the neutron flux and the amount of radio-active isotope present in the sample, it is at least theoretically possible to determine the isotope amount by direct activity measurement. But due to uneven flux distribution in the reactor and inexact overall efficiency of radiation detector it is not a reliable method.

Alternately, quantitative analysis by radio-activation techniques follows a procedure in which the specimen and a known weight of the element being determined are bombarded under the same reactor conditions. The activities are subsequently measured, the concentration of the element in the unknown being calculated as a simple ratio of the radio-activity of the element of interest produced in the sample to the radio-activity produced in the standard.

A measurable amount of radio-activity from one or more radio-isotopes of the element is produced when a stable isotope (or isotopes) of the element is bombarded. The activity, A, present at a

time, t_o, after the start of the bombardment, can be calculated from the expression

$$A = N \phi \sigma S$$

where A = the amount of radio-activity in disintegrations per second, N = the number of atoms of the target nuclide, ϕ = the thermal neutron flux per square centimeter per second, σ = the activation cross-section (probability) for the reaction in square centimeters per atom (usually expressed in barns), and S = the saturation factor, $\left\{1 - \exp(-\lambda t_o)\right\}$, or the ratio of the amount of radio-activity produced in time, t_o, to that produced in infinite time. The decay constant, λ, is related to the half-life, $T_{1/2}$, of the radionuclide produced ($\lambda = \frac{0.693}{T_{1/2}}$). The activity of the sample at a time, t, measured from the instant the irradiation is stopped is given by

$$A = \sigma \phi N \left\{1 - \exp(-\lambda t_o)\right\} \exp(-\lambda t)$$

All the disintegrations are not detected, however, only a small fraction, g, of the energy emitted will reach the detecting crystal and a fraction, p, of these will be absorbed by the crystal. The observed counting rate is even smaller because the gamma radiation of a particular energy is but a fraction, f, of the disintegrations of an active isotope. Assuming all the absorbed gamma rays are counted then the counting rate, C will be

$$C = A\ f\ g\ p.$$

Gamma energy detection

The three important ways in which gamma rays interact

with an absorbing material are photoelectric effect, Compton effect and pair-production. In the photoelectric effect a complete elastic transference of energy from the gamma ray to an orbital or conduction electron occurs. In the Compton scattering the electron only makes a partial absorption of the gamma energy while the gamma ray is elastically scattered. Pair-production happens when gammas of energy over 1·02 Mev pass near a nucleus and are annihilated by giving birth to an electron-positron pair.

When gamma rays interact with a scintillation crystal, the absorbed part of the energy is converted into light impulses. These light impulses are made to fall upon the cathode of a photo-multiplier tube for primary amplification. The output from the photo-multiplier tube is led to a cathode follower to produce pulses of negative potential proportional to absorbed energy. These pulses are amplified in a linear amplifier and counted in a pulse-height analyser.

INSTRUMENTATION

The gamma-ray spectrometer used to measure activities in this investigation is made by Philips Industries Limited. The components are:

1. PW 4111, a scintillation probe consisting of a 25 millimeter diameter scintillation crystal (thallium activated NaI) for detecting the radiation, a photo-multiplier tube with 11 dynodes, and a cathode follower.

2. PW 4071, a pre-amplifier designed as an impedance matching link between the radiation detector PW 4111 and the main amplifier PW 4072.

3. PW 4022, a high voltage pre-amplifier unit which can supply the voltage needed by the radiation detector, PW 4111, to a maximum of 2,500 volts.

4. PW 4029, a stabilized supply unit designed primarily to provide the linear amplifier PW 4072 with power. The deviation is less than $\pm$ 0·01 percent of the mains fluctuation.

5. PW 4072, a linear amplifier, which amplifies pulses with varying amplitude. The unit amplifies pulses having gain of 2400 and input attenuation facility of 1X, 2X, 4X, 8X and 16X.

6. PW 4082, a single channel pulse-height analyser to separate pulses with different amplitudes and, thereby, to analyse

the energy spectrum of radiation. On threshold-discrimination setting all pulses above the adjusted voltage are counted. Using channel-discrimination all pulses within a set 'window' of voltages are recorded. The channel-width is adjustable to 1,2,4,8,12,16,20, 24,28 or 32 volts. The center of the voltage range within the channel is the channel-height and is adjustable to any value between 4 and 100 volts.

7. PW 4032, a universal scaler, used for counting pulses up to a maximum of 4×10^5. Settings for total counts are 1,2, or 4 times 10, 10^2, 10^3, 10^4 or 10^5.

8. PW 4052, a preset-count unit, used for measuring the time during which a predetermined number of pulses occur

Counting Castle

The sample whose activity was to be measured was placed on a shelf inside a lucite box kept fixed inside a 2-inch thick lead castle. The scintillation probe projected through a hole in the top of the lead castle and rested on a ridge just above the lucite box. 14 shelf positions were available in the lucite box whereon the sample could be placed at distances of from 0·5 to 14 centimeters from the crystal base. The relative count rates for different shelf positions are shown in figure 4. The active samples were stored behind 2-inch lead shielding, away from the experiments' neighbourhood. The flow diagram showing the connections between the units of the gamma-ray spectrometer and their relations with the active sample in the lead castle has been given in figures 2 and 3.

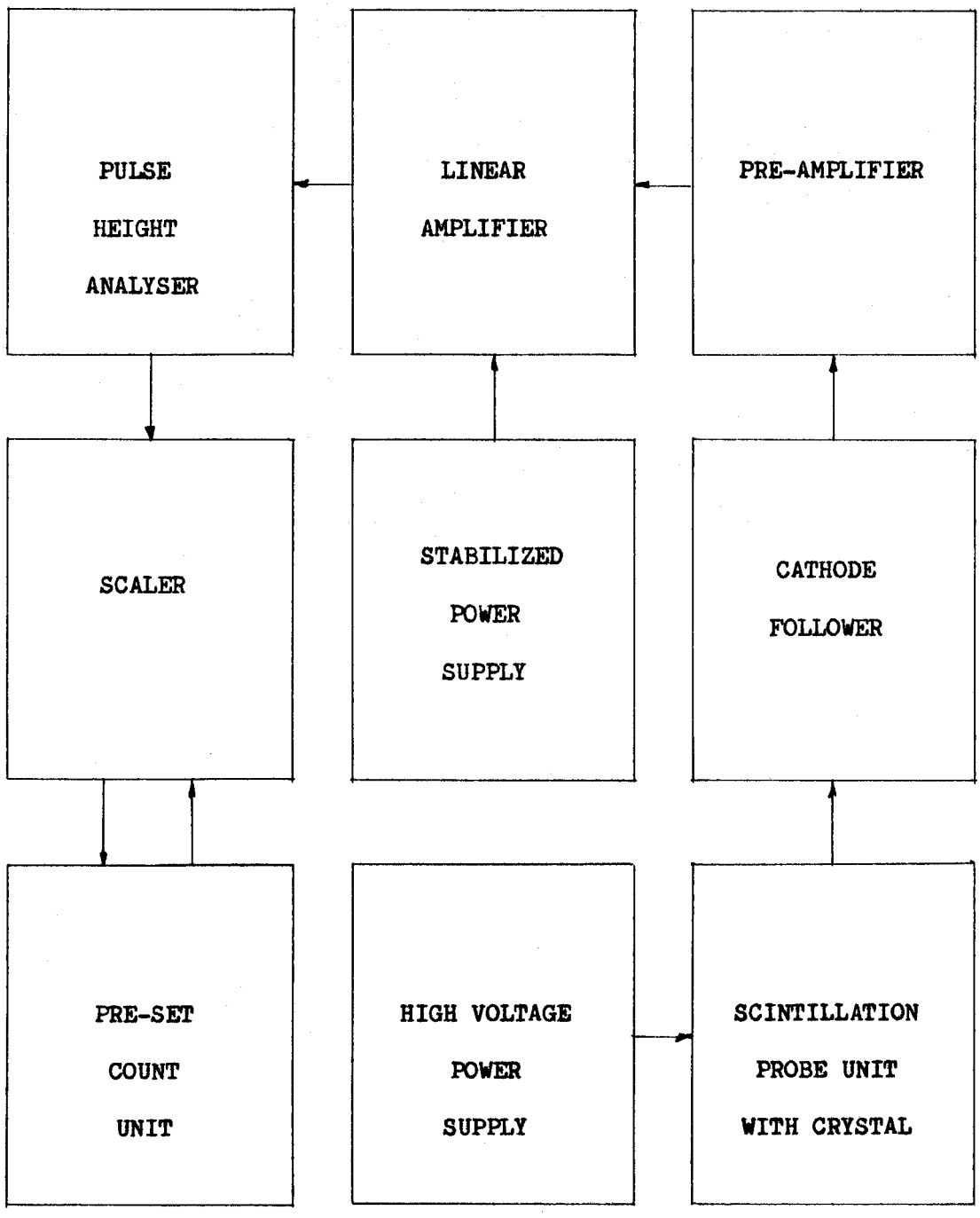

Figure 2. Flow diagram for the gamma-ray spectrometer.

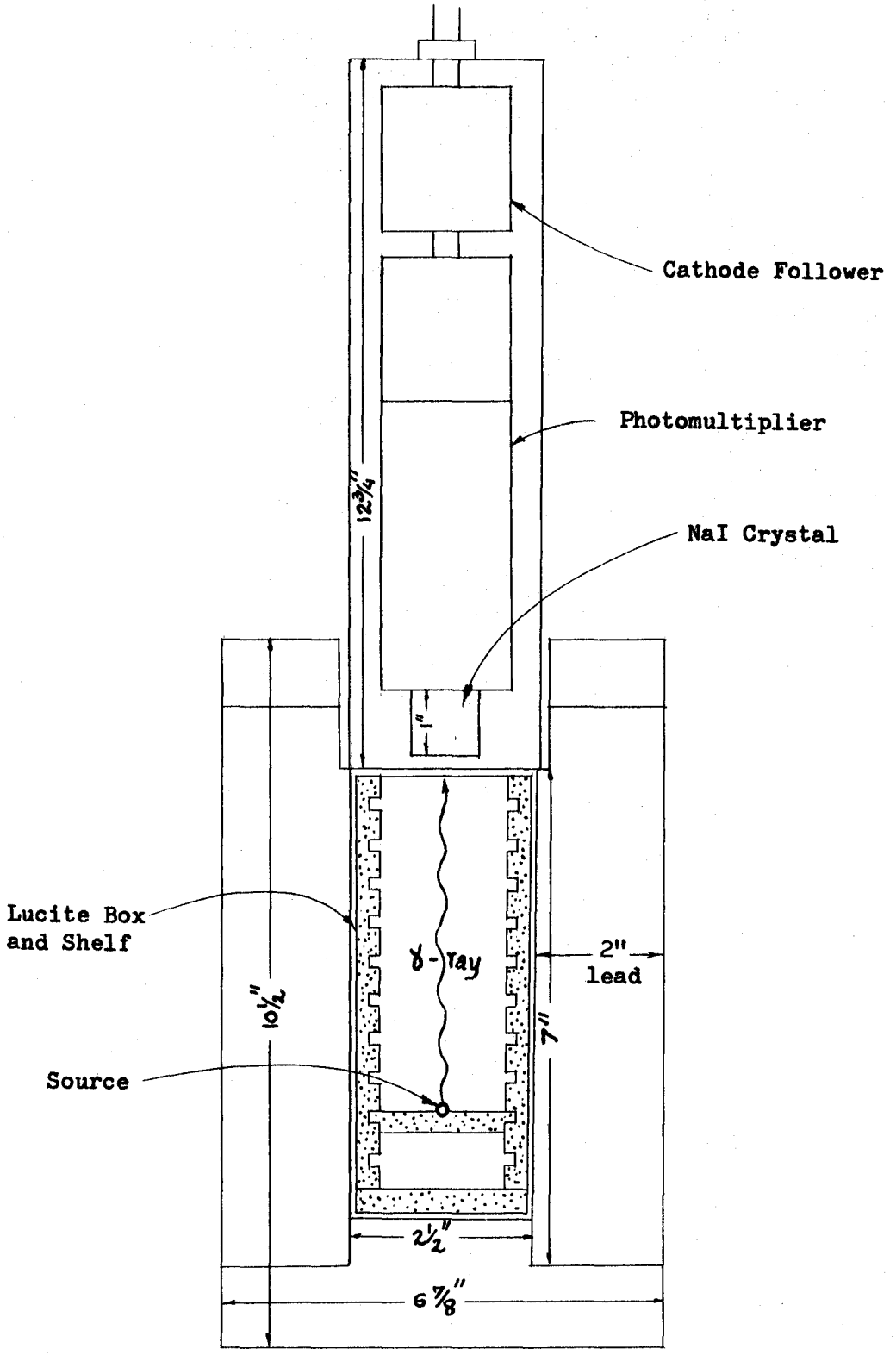

Figure 3. Section through counting castle showing scintillation probe unit and source geometry for diffusion samples.

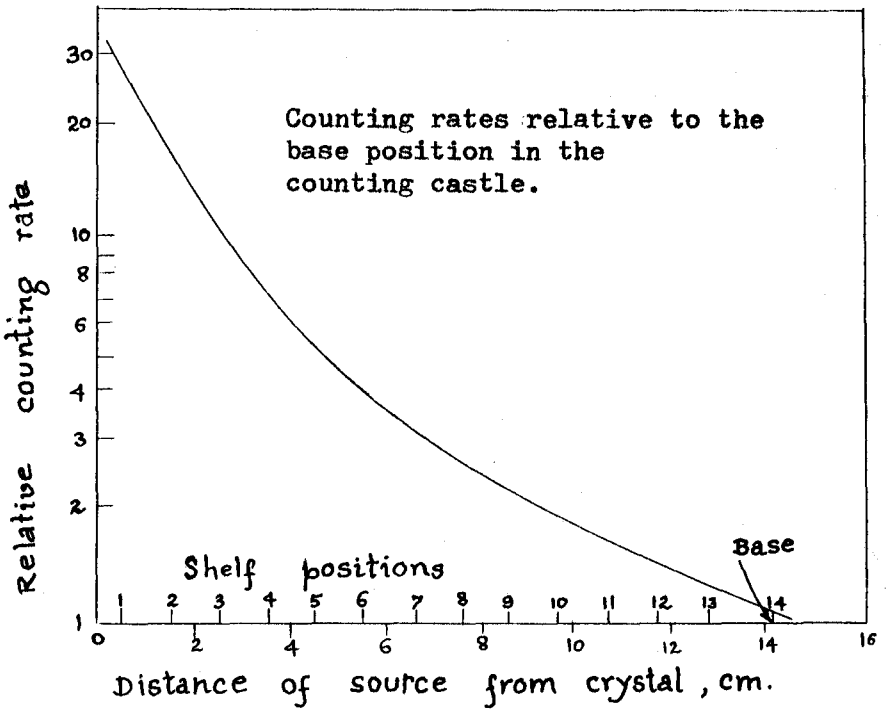

Figure 4. Relative counting rates from a given point source on different shelf positions in the counting castle. (Mason[13])

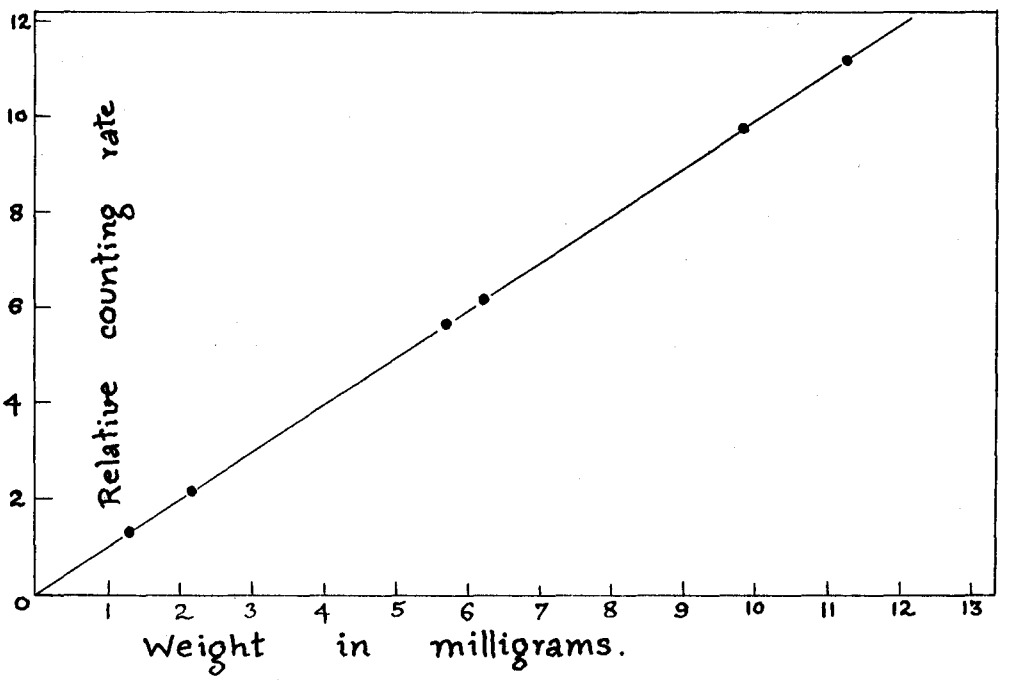

Figure 5. Linearity plot of the spectrometer for different weights of copper isotope.

Instrumental check-ups

The linearity of the spectrometer over the useful range was checked by counting different weights of 3·32 percent Aℓ-Cu alloy irradiated together. This has been shown in figure 5. The stability of the spectrometer over a period of time was also checked.

Copper and Zinc Activity

Important nuclear data for the isotopes of copper and zinc is given in Table 1; and gamma spectra determined from pure metals irradiated in the McMaster reactor at a neutron flux of 10^{13} $n/cm^2 sec$ are shown in figures 6 and 7 for copper and zinc.

It is noticed from the two spectra that the 1·35 Mev photo-peak of copper and the 1·114 photo-peak of zinc are nearly congruent on their amplitude setting. Both of them start at almost the same voltage. Taking advantage of relative differences in the half-lives of copper and zinc (12·8 hours for Cu and 245 days for Zn), zinc activity can be measured at the threshold setting on the dip of the spectrum (i.e. where the two photo-peaks start) after letting the copper activity decay completely by waiting approximately 12 days. The copper activity is measured at the same threshold setting without any appreciable interference by the zinc (which is about 0·15 percent of the copper activity). Since activated aluminum has a half-life of only 2·3 minutes, the experiment is not influenced by it.

TABLE 1

Nuclear Data for Cu, and Zn

Element	Cu	Zn
Isotope measured	64	65
Percent abundance of the radio-nuclide	69·0	48·89
Thermal neutron cross-section, σ barns	4·4	0·44
Half life of activated isotope ($T_{1/2} = 0{\cdot}693/\lambda$)	12·8 hr.	245 days
Energies of gamma rays emitted in Mev.	1·35, 0·5	1·114

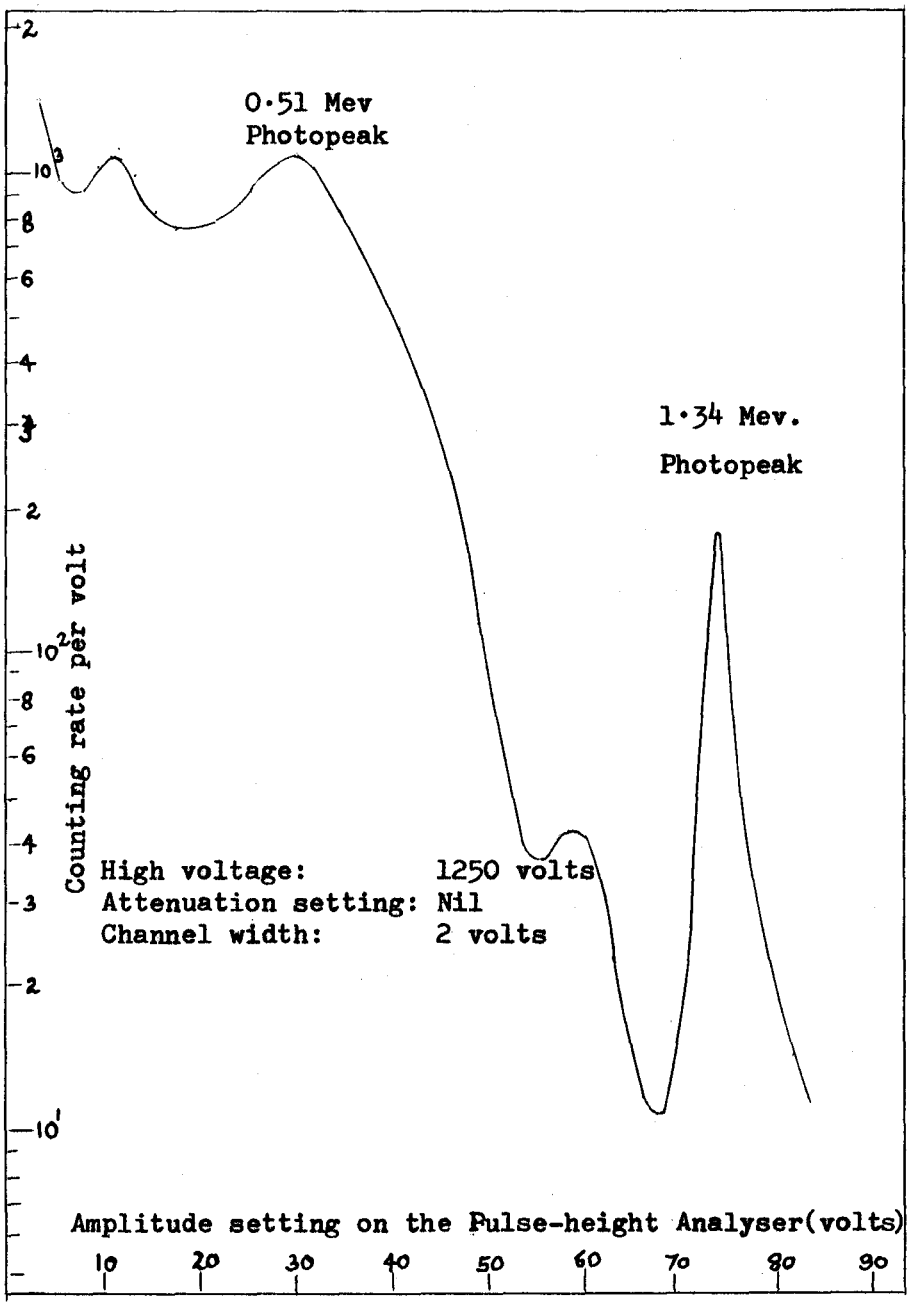

Figure 6. Specimen of Cu 64, obtained experimentally from a sample of pure copper (99-98%) irradiated in the McMaster reactor.

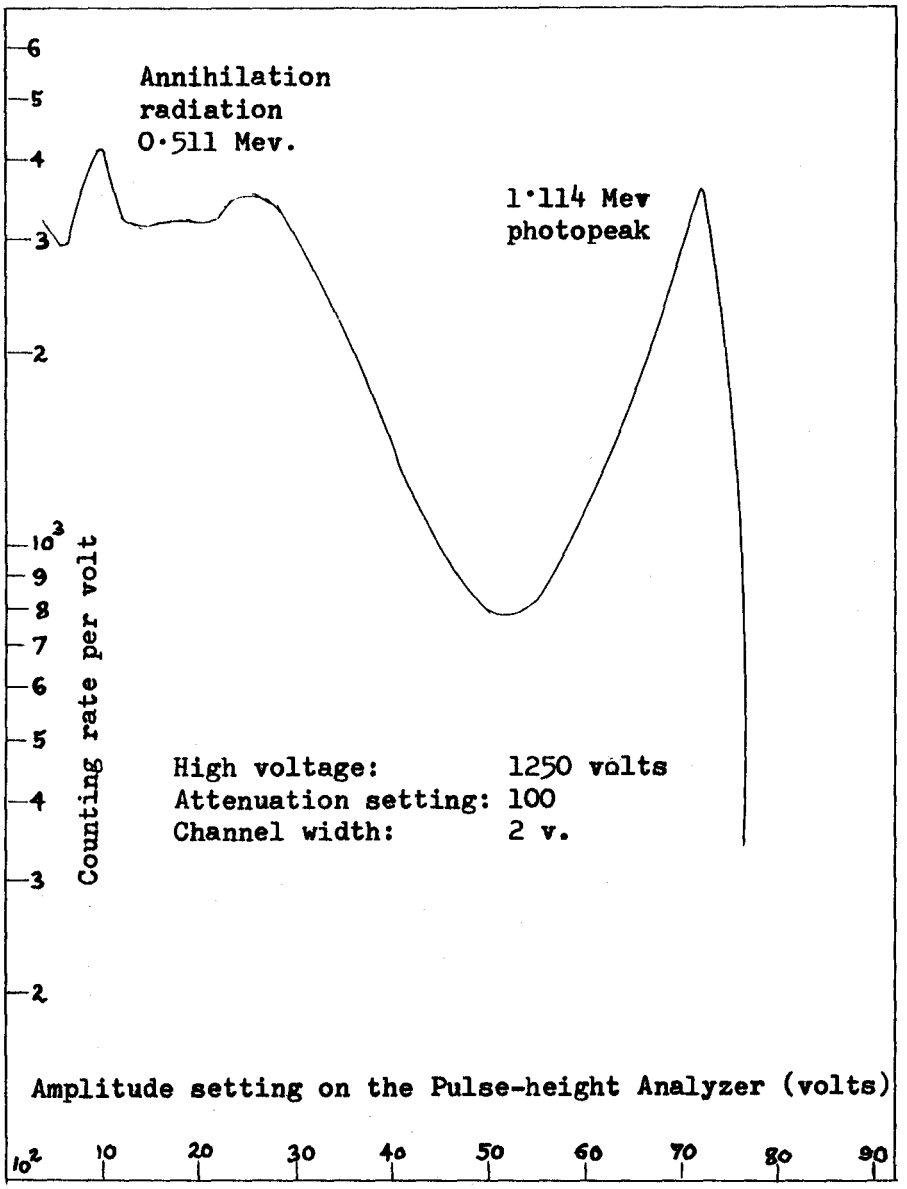

Figure 7. Specimen of Zn, obtained experimentally from a sample of pure Zn (99·99) irradiated in the McMaster reactor.

EXPERIMENTAL PROCEDURE AND RESULTS

To assure obtaining single-phase diffusion at the temperature of anneal (503·6°C), the aluminum rich corner of the Aℓ-Zn-Cu constitution-diagram was studied. The only ternary isotherm[19] available in the literature was at 460°C. From the binary phase diagrams[19] for Aℓ-Cu and Aℓ-Zn an approximate extrapolation of the α-phase extension was done to the 503·6°C isotherm (see figures 8,9,10,11). This isotherm was kept in mind in preparing alloy compositions for the diffusion couples.

Binary and ternary aluminum alloy ingots were cast and then homogenized in a muffle furnace. Above 1/4 inch from all the sides of each ingot was machined off to correct any defect due to inverse segregation or to zinc loss during annealing. The ingots were then rolled to about 3/4 inch thickness and again homogenized. Cylinders of the alloys about 1/2 inch in diameter and 1/2 inch in length were cut, and freshly cut faces of the pairs of cylinders were clamped together tightly, keeping the interval between the final cut on the first half of a couple and the clamping of the two halves together to a minimum (less than a minute) to reduce the amount of oxidation at the interface. The tightly clamped assembly of diffusion couples was enclosed in an iron box, half filled with ingot chips (to cut down the evaporation loss of zinc). The box was then placed in a forced convection tempering oven* for a period of $1{\cdot}3077 \times 10^6$ seconds (roughly 2 weeks).

---

* Blue M Mechanical Convection Oven.

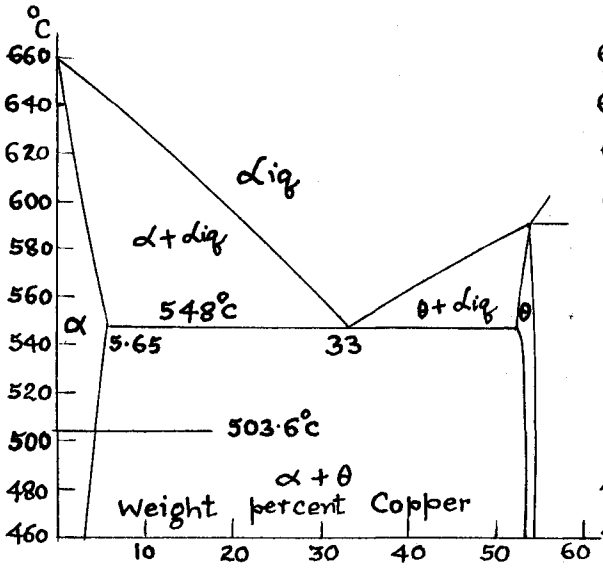

Figure 8. Binary diagram for Aℓ-Cu.

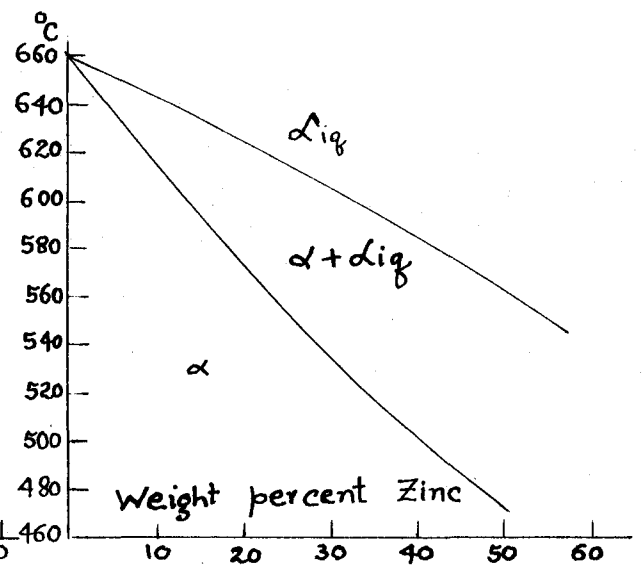

Figure 9. Binary diagram for Aℓ-Zn.

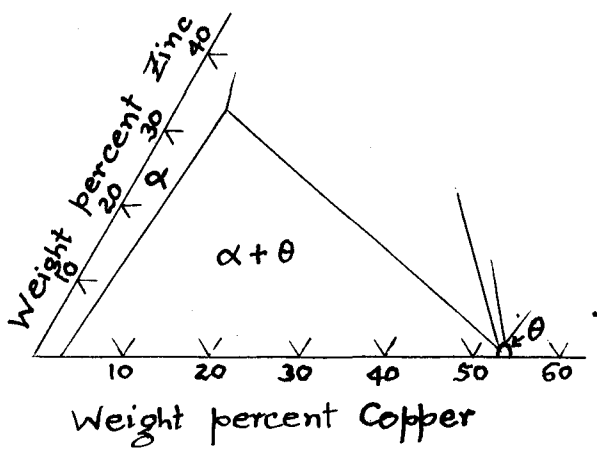

Figure 10. Aℓ-Cu-Zn 460°C Isotherm for the Aℓ-rich corner.

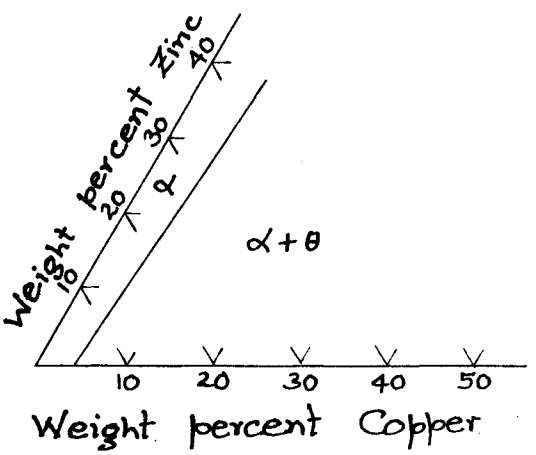

Figure 11. Aℓ-Cu-Zn 503·6°C Isotherm for the Aℓ-rich corner extrapolated.

The average diffusion annealing temperature was 503·6°C, controlled to ± 1·5°C by means of a commercial proportioning control system*. The recording was done with the help of an iron-constantum thermocouple which was connected to a dummy couple in the assembly inside the furnace; the thermocouple was standardized against a thermocouple (Pt - Pt 10% Rh) certified by the National Research Council, Ottawa.

Preparation of samples for irradiation

The couples, on their removal from the oven were water quenched and taken out of the clamp. They were then turned down to about 3/8-inch in diameter and lined up in a collet until the interface appeared to be perpendicular to the center line of the lathe bed within about a thousandth of an inch. The lining-up was performed by first turning down a couple a little and then etching in Tucker's etch (15% HF, 45% HCℓ, 15% HNO_3 and 25% H_2O) so that the interface was visible. This was checked for correct alignment in the lathe collet with the help of a fine pointer and a magnifying glass. The couple was then cut to a point which was a few thousandths from the point where the first sample was to be collected. The distance from this edge to the interface was now measured with a micrometer eyepiece. The couple was next replaced in the collet, the alignment was checked and samples were taken at mean distances of 1,3,5,9,13,19,25, 33,43,57,75 and 95 thousandths of an inch on either side of the interface with cuts made of 2 thousandths of an inch width. The standard alloy samples were collected from the semi-infinite zone on

* Blue M Electric Co., Blue Island, Illinois, U.S.A.

one side of the couple.

Samples of from 6 to 10 milligrams were weighed on a Mettler microgramatic balance, and packed in preglazed silica capsules (20 millimeter long, 1·5 millimeter internal diameter and 2·5 to 3 millimeter external diameter) before they were sealed off. The weighing was always performed by taking the difference in weight of the empty capsule and the packed one before sealing. The sealed capsules were placed in a spacer made of super-purity aluminum prior to irradiation. The relative positions of unknown samples and of standard samples are shown in figure 12. The spacer was then rolled in aluminum foil and it was ready for irradiation.

Measurement of activity of the samples

The period of irradiation and the suitable neutron flux were calculated for each individual package knowing the average values of compositions in it with the help of Table 1, so that, measurable amount of zinc activity would be produced without raising the copper activity too high. After the irradiation of a package, the capsules were wiped with clean tissue paper to remove any sodium* contamination and counted. All the countings were done using a photomultiplier voltage of 1250 volts. The maximum counting error was kept to 1 percent by setting the preset count for 1×10^4 and higher. The cosmic background was low and almost stationary. The copper count was always corrected for zinc background and for time lag while counting.

---

* Sodium contamination from perspiration during handling.

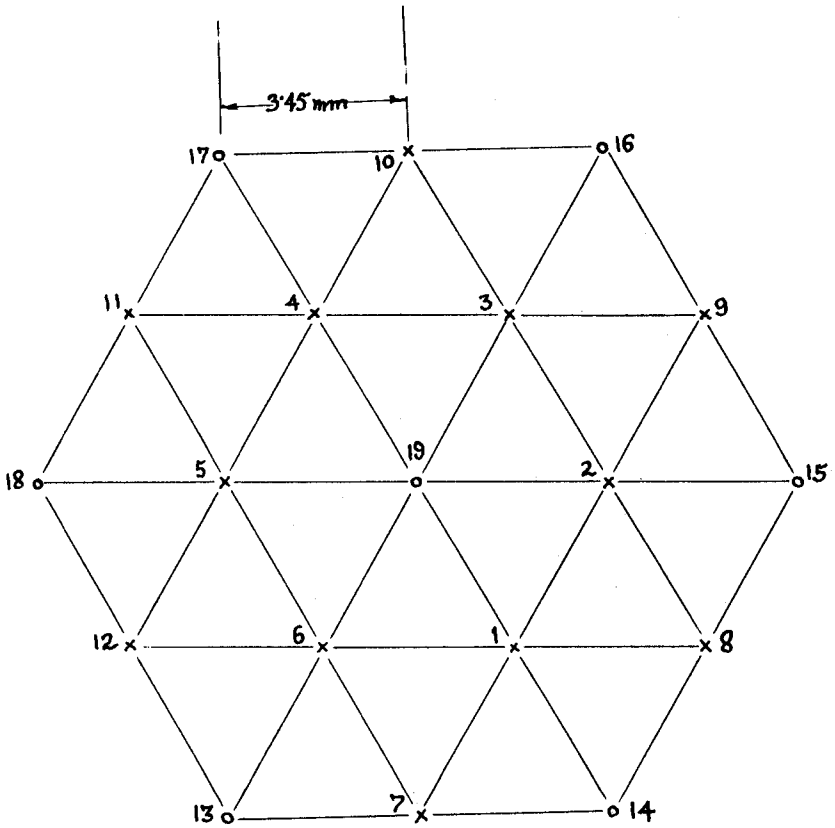

o Position of a standard sample

x Position of an unknown sample

Figure 12. Relative positions of the unknown samples and the standards in the aluminum spacer.

Results of activity measurements

The sequence of steps used in determining the weight percentage of an isotope in a sample from the measured activity are given in the following.

(i) The uncorrected counting rate, A_u, for each sample was calculated according to the relation

$$A_u = \frac{C}{w\Delta t}$$

where C is the number of threshold counts, w is the weight of the sample and Δt is the time taken for C counts.

(ii) Background correction, B, was made for cosmic activity according to

$$A_c = A_u - B$$

where A_c is the corrected activity.

(iii) The activity was corrected to some arbitrary reference time for a set of samples using the relation

$$A = A_c \exp(\lambda \tau)$$

where λ is the decay constant for the element concerned and τ is the time measured from the arbitrary reference time. This procedure was followed in counting copper activity but was omitted in the case of zinc because of its very long half-life.

(iv) The standard activity for a position containing a sample of unknown composition in the aluminum spacer was determined from the activities of the standard samples by parabolic interpolation.

(v) The weight percent of the isotope in the unknown sample was measured as a percentage of the weight percent of the isotope in the standard samples from the knowledge of the interpolated standard activity at a particular position according to

$$P = \frac{W}{W'} \times 100 = \frac{A}{A'} \times 100 ,$$

where P is the required percentage, W' is the weight percent of the isotope in the standard sample, W is the weight percent of the isotope in the unknown sample, A' is the corrected specific standard activity, at a particular time, interpolated for the position of the unknown sample and A is the corrected specific activity of the unknown sample at the particular time.

The copper and zinc penetration curves for binary couples, (3·32 percent copper in aluminum versus pure aluminum and 12·6 percent zinc in aluminum versus pure aluminum) are plotted in figures 13 and 14. Both the curves are symmetric and the two diffusion constants seem to be fairly independent of concentration. This is shown for copper and zinc on the probability graphs in figures 15 and 16. The diffusion coefficients for copper and zinc at 503·6°C have been calculated to be approximately $4{\cdot}54 \times 10^{-10}$ cm^2/second and $2{\cdot}905 \times 10^{-9}$ cm^2/second respectively as illustrated in the figures 13 and 14. The method of calculation is discussed in Appendix A.

The reported[20] values of the binary diffusion coefficients at 503°C for copper and zinc for the aforementioned concentrations are $3{\cdot}6 \times 10^{-10}$ cm^2/second and $2{\cdot}52 \times 10^{-9}$ cm^2/second respectively. These

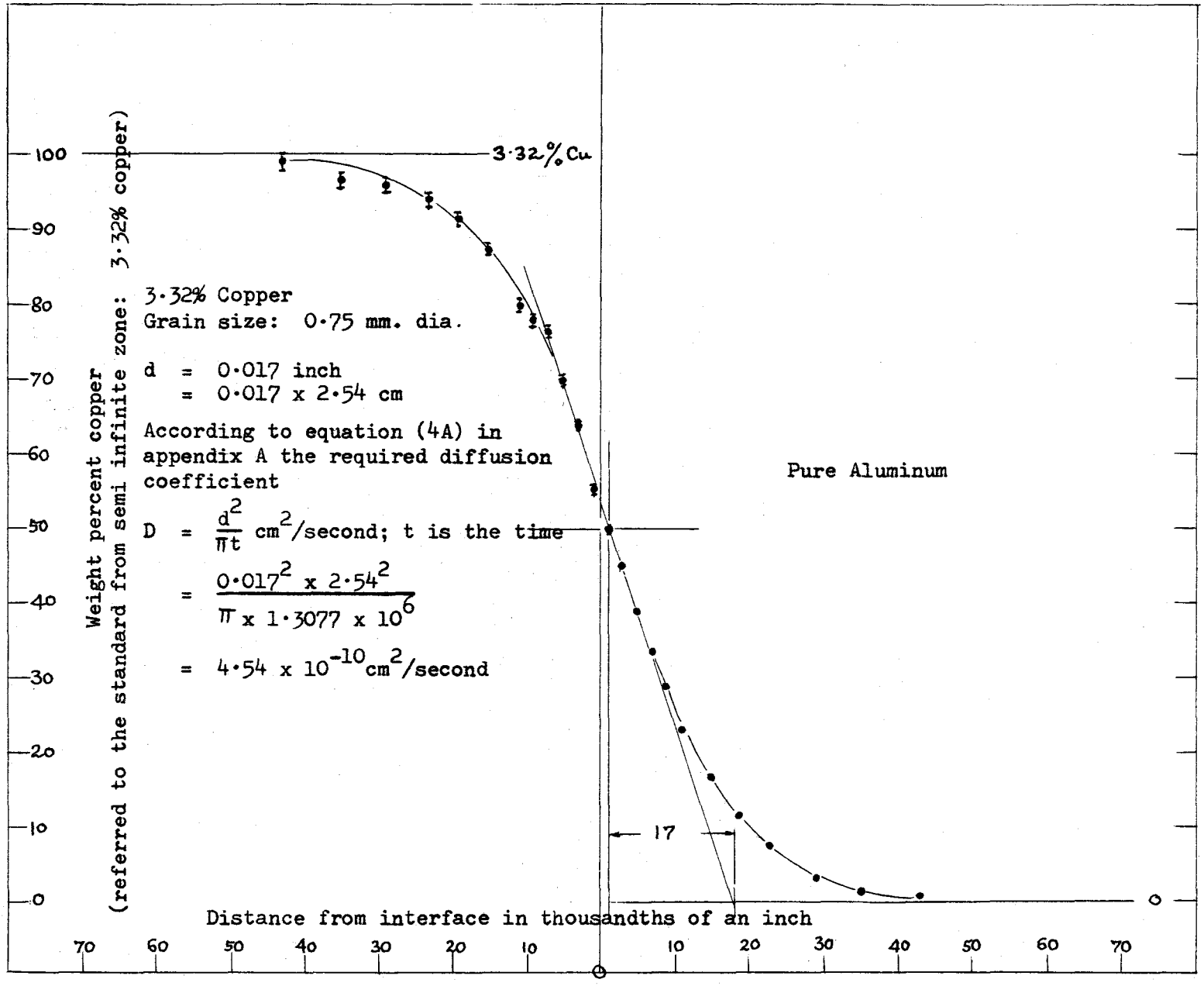

Figure 13. Copper penetration in a binary Al-Cu couple [3·32 percent Cu in Aluminum versus pure aluminum] annealed at 503·6°C for 1·3077 x 10^6 seconds.

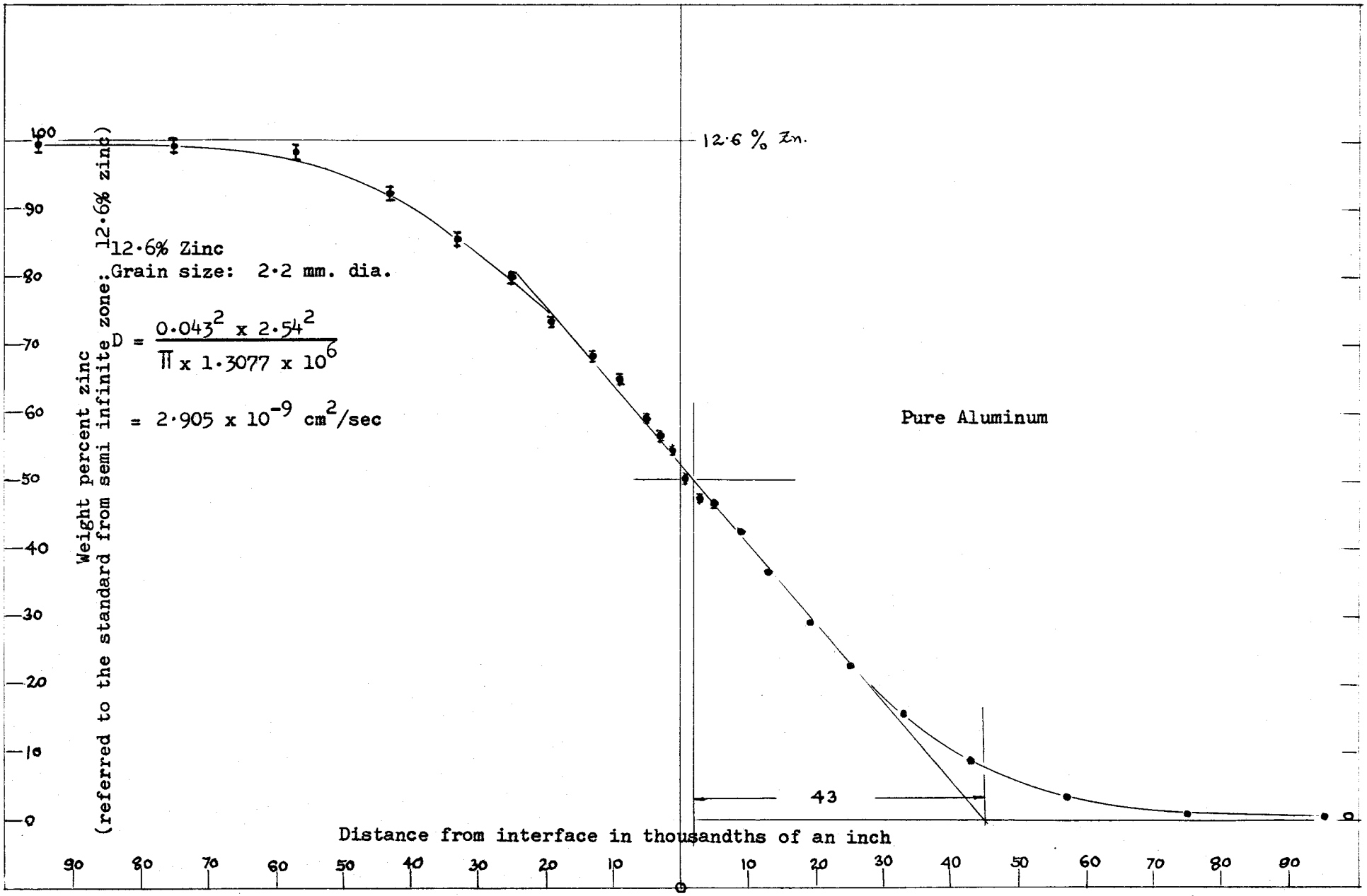

Figure 14. Zinc penetration in a binary Aℓ-Zn couple [12·6 percent zinc in Aluminum versus pure Aluminum] annealed at 503 6°C for 1·3077 x 10^6 seconds.

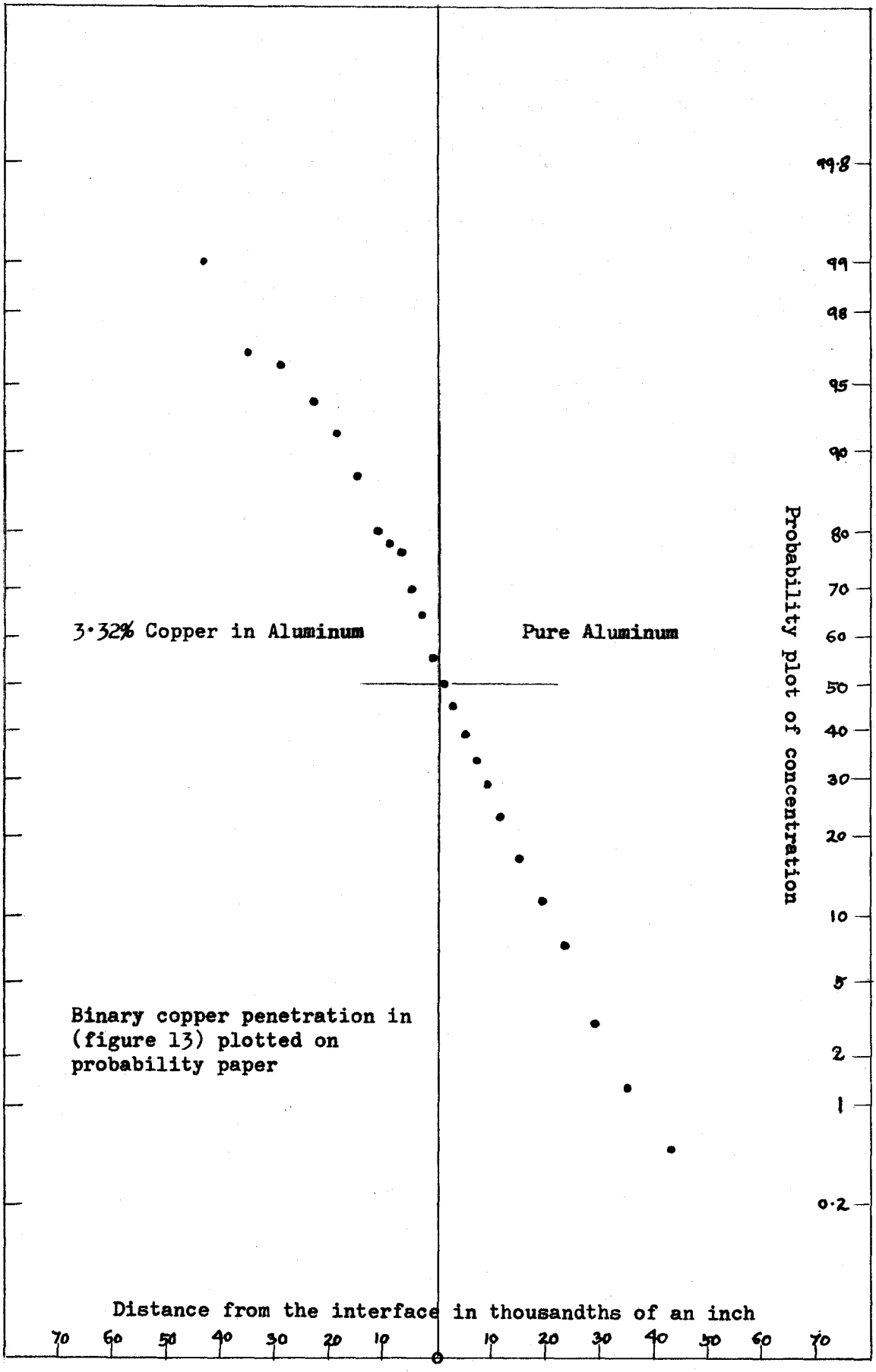
3·32% Copper in Aluminum
Pure Aluminum
Binary copper penetration in (figure 13) plotted on probability paper
Probability plot of concentration
99·8
99
98
95
90
80
70
60
50
40
30
20
10
5
2
1
0·2
Distance from the interface in thousandths of an inch
70 60 50 40 30 20 10
10 20 30 40 50 60 70

Figure 15

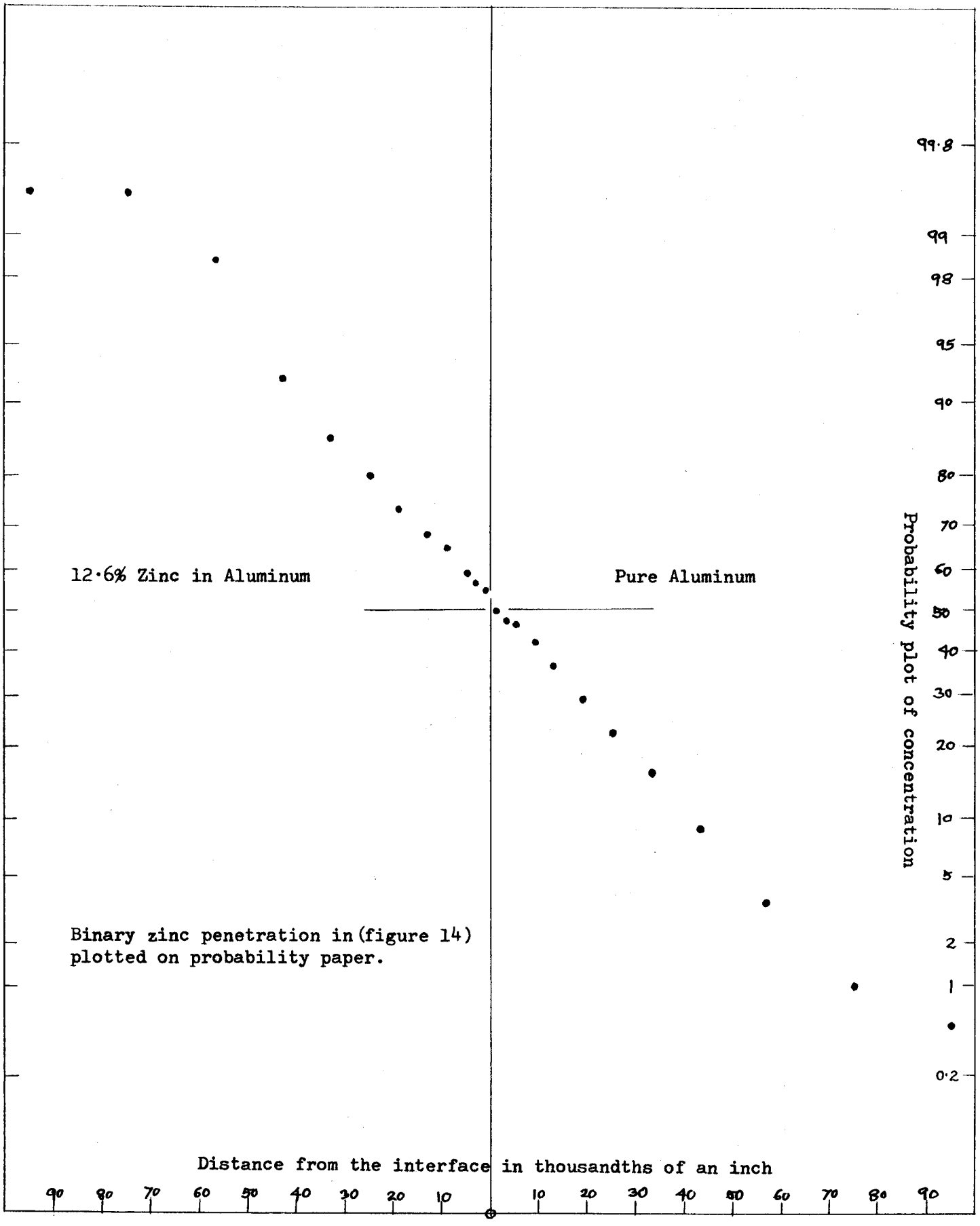

Binary zinc penetration in (figure 14) plotted on probability paper.

Figure 16

values compare favorably with those obtained in this investigation. The grain sizes on both sides of the interface for each couple are noted on the appropriate penetration diagrams.

The copper penetration in the presence of zinc (3·66 percent copper and 11·8 percent zinc in aluminum versus 12·6 percent zinc in aluminum) is shown in figure 17. The same plottings on the probability graph 18 exhibit concentration dependence. The calculated diffusion coefficient for copper along its own gradient in presence of zinc is about $1{\cdot}232 \times 10^{-9}$ cm^2/second. Finally the effect of a copper gradient on zinc diffusion is shown in figure 19. The couple used was 3·66 percent copper and 11·8 percent zinc in aluminum versus 12·6 percent zinc in aluminum. On substituting $D_{22} = 1{\cdot}232 \times 10^{-9}$ cm^2/second and $D_{11} = 2{\cdot}905 \times 10^{-9}$ cm^2/second in equation (57), the best fit to the results plotted in figure 19 are obtained for $D_{12} = 1{\cdot}65 \times 10^{-9}$ cm^{2}second.

Zinc penetration in the presence of copper (11·8 percent zinc and 3·66 percent copper in aluminum versus 3·32 percent copper in aluminum) is shown in figure 20. The symmetry of zinc penetration is illustrated in figure 21. The calculated D_{11} for this curve is $3{\cdot}4 \times 10^{-9}$ cm^2/second. Substituting $D_{11} = 3{\cdot}4 \times 10^{-9}$ cm^2/second, $D_{22} = 1{\cdot}232 \times 10^{-9}$ cm^2/second and $D_{12} = 1{\cdot}65 \times 10^{-9}$ cm^2/second in the approximate relation (50)

$$X_1 D_{21} D_{11} \cong X_2 D_{12} D_{22}$$

the value obtained for D_{21} is approximately $9{\cdot}66 \times 10^{-11}$ cm^2/second. X_1, X_2, are the mean mole fractions at the interface. The value has

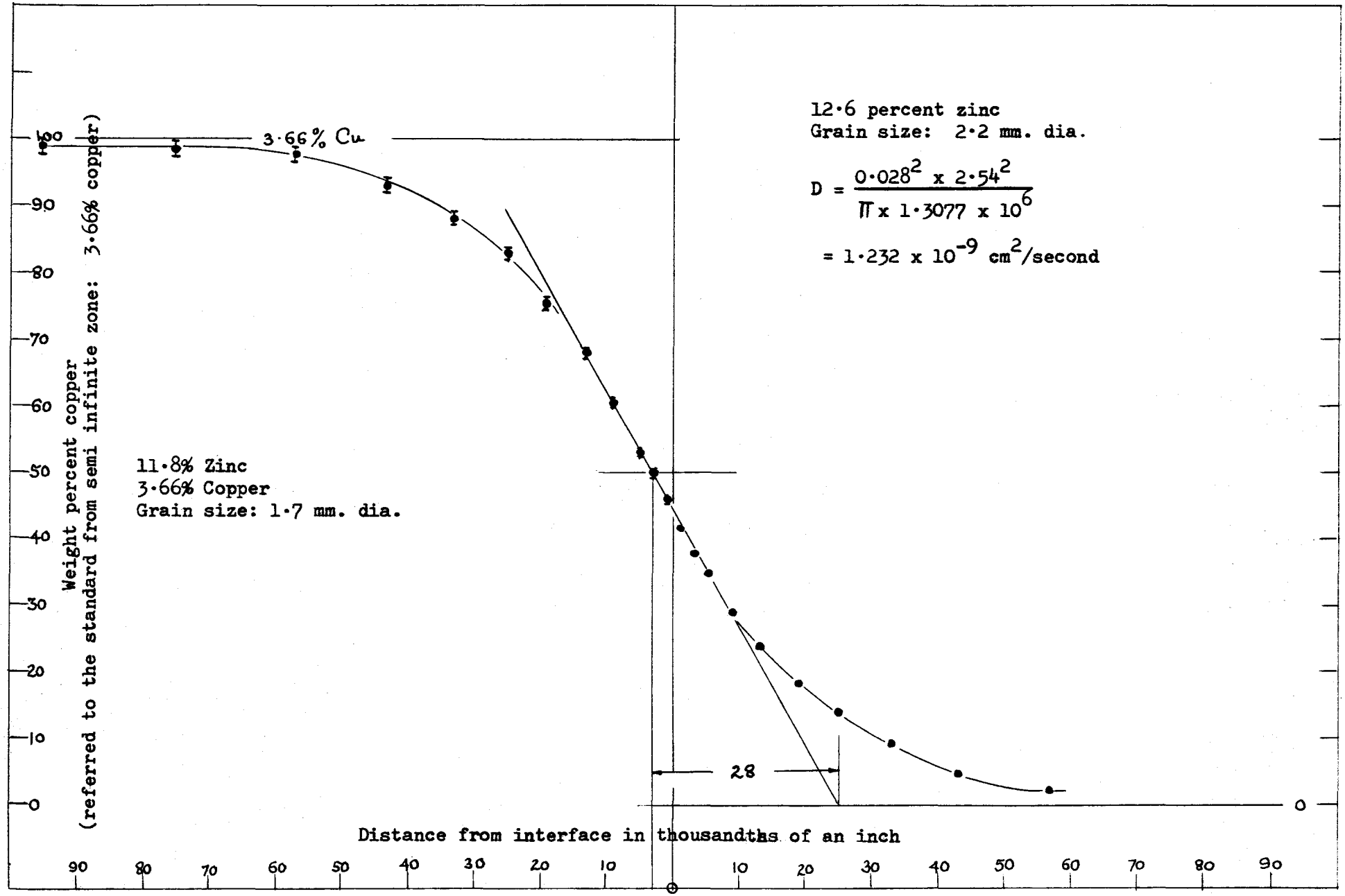

Figure 17. Copper penetration in a couple made of 3·66 percent copper and 11·8 percent zinc in aluminum versus 12·6 percent zinc in aluminum.

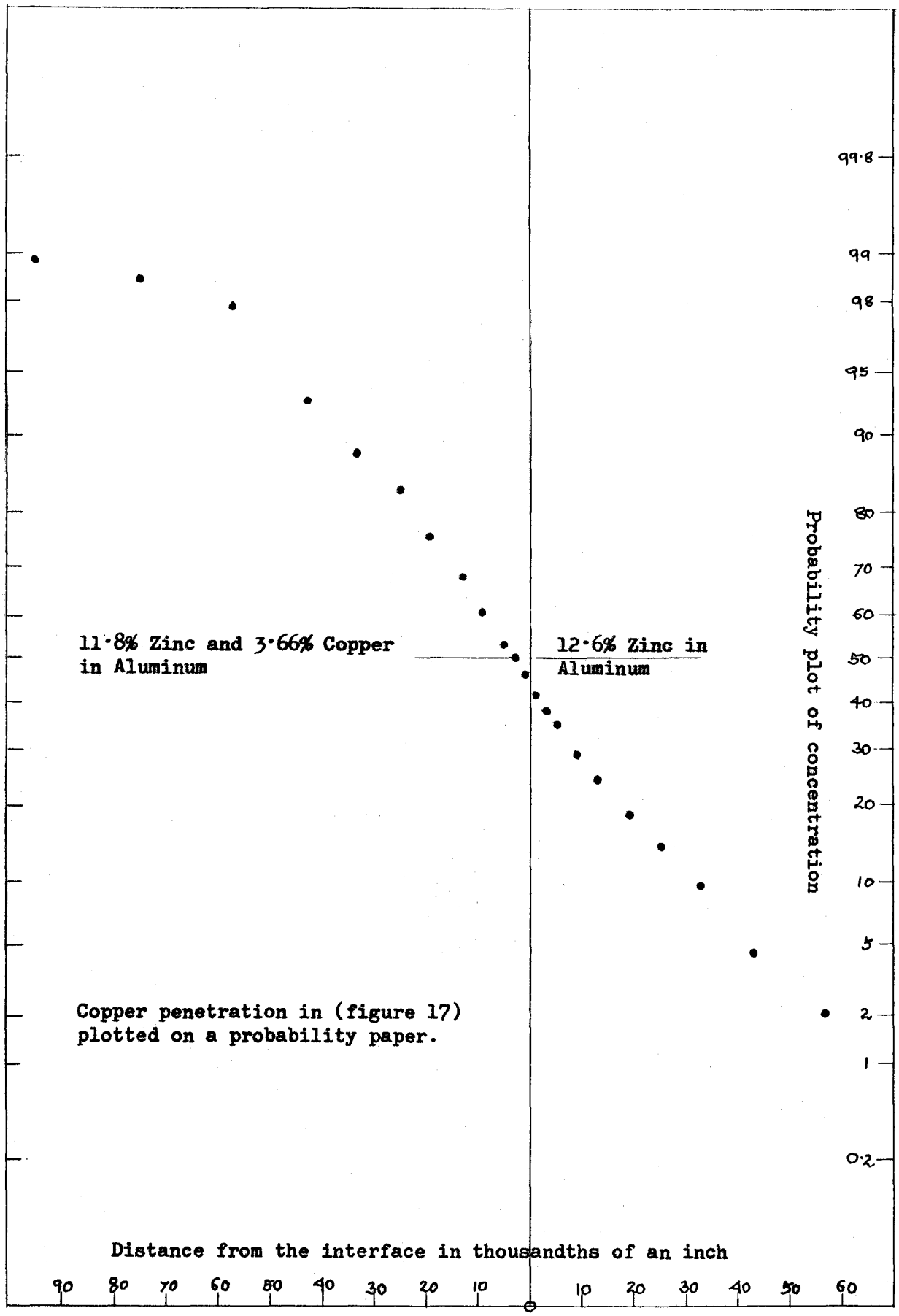
11·8% Zinc and 3·66% Copper in Aluminum
12·6% Zinc in Aluminum
Copper penetration in (figure 17) plotted on a probability paper.
Probability plot of concentration
99·8
99
98
95
90
80
70
60
50
40
30
20
10
5
2
1
0·2
Distance from the interface in thousandths of an inch
90 80 70 60 50 40 30 20 10
10 20 30 40 50 60

Figure 18

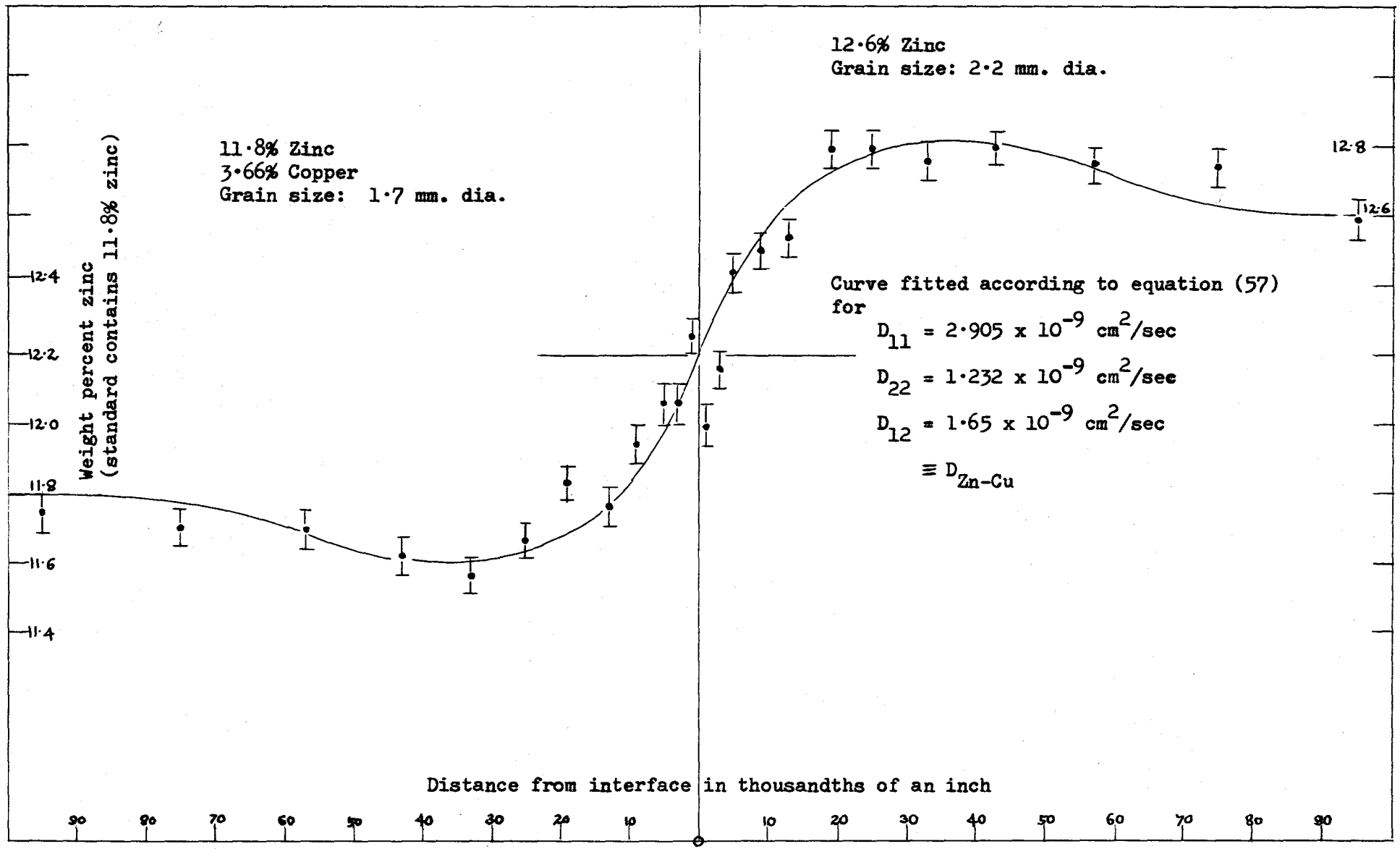

Figure 19. Effect of copper gradient on zinc diffusion.

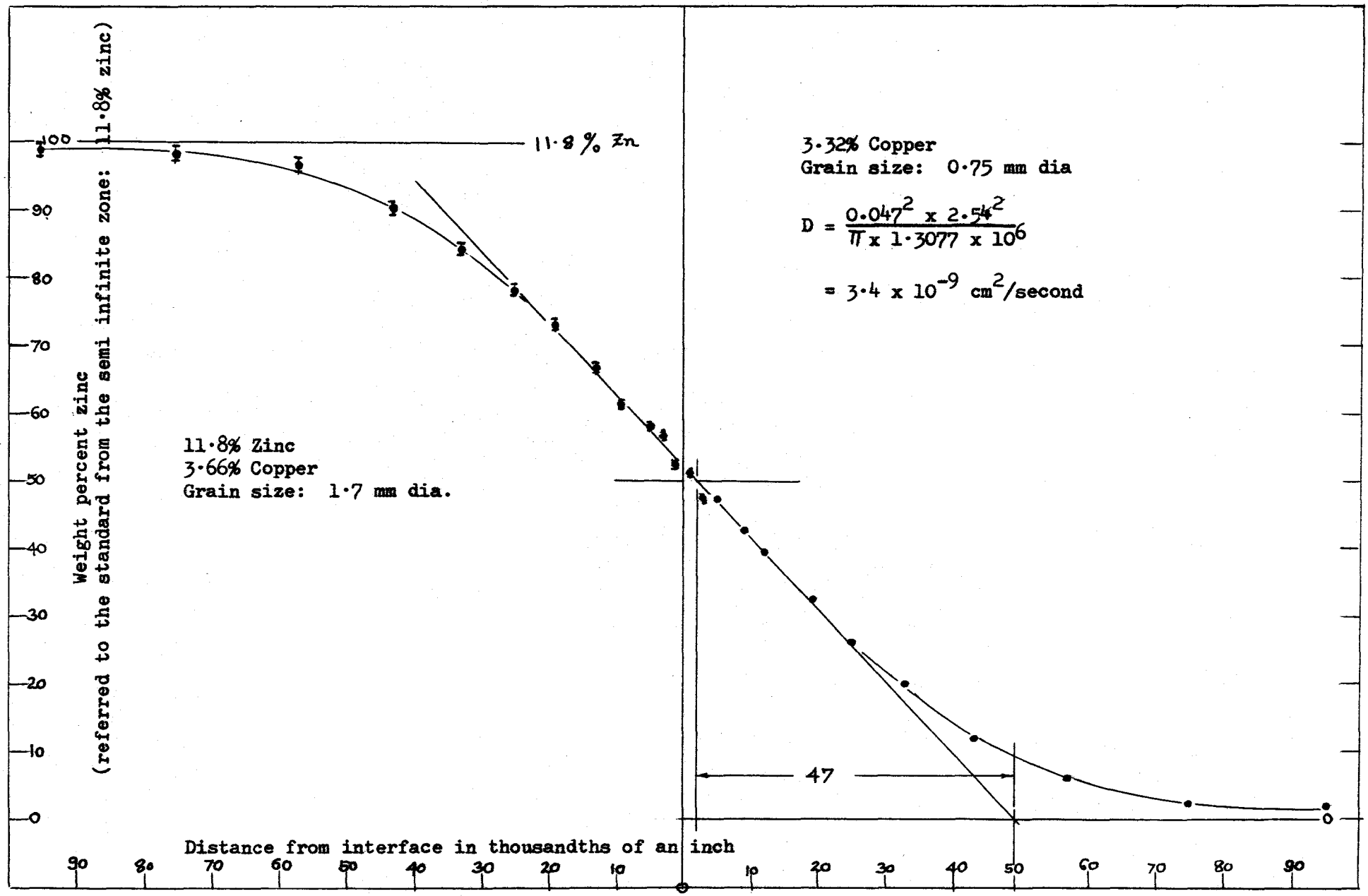

Figure 20. Zinc penetration in the presence of copper.

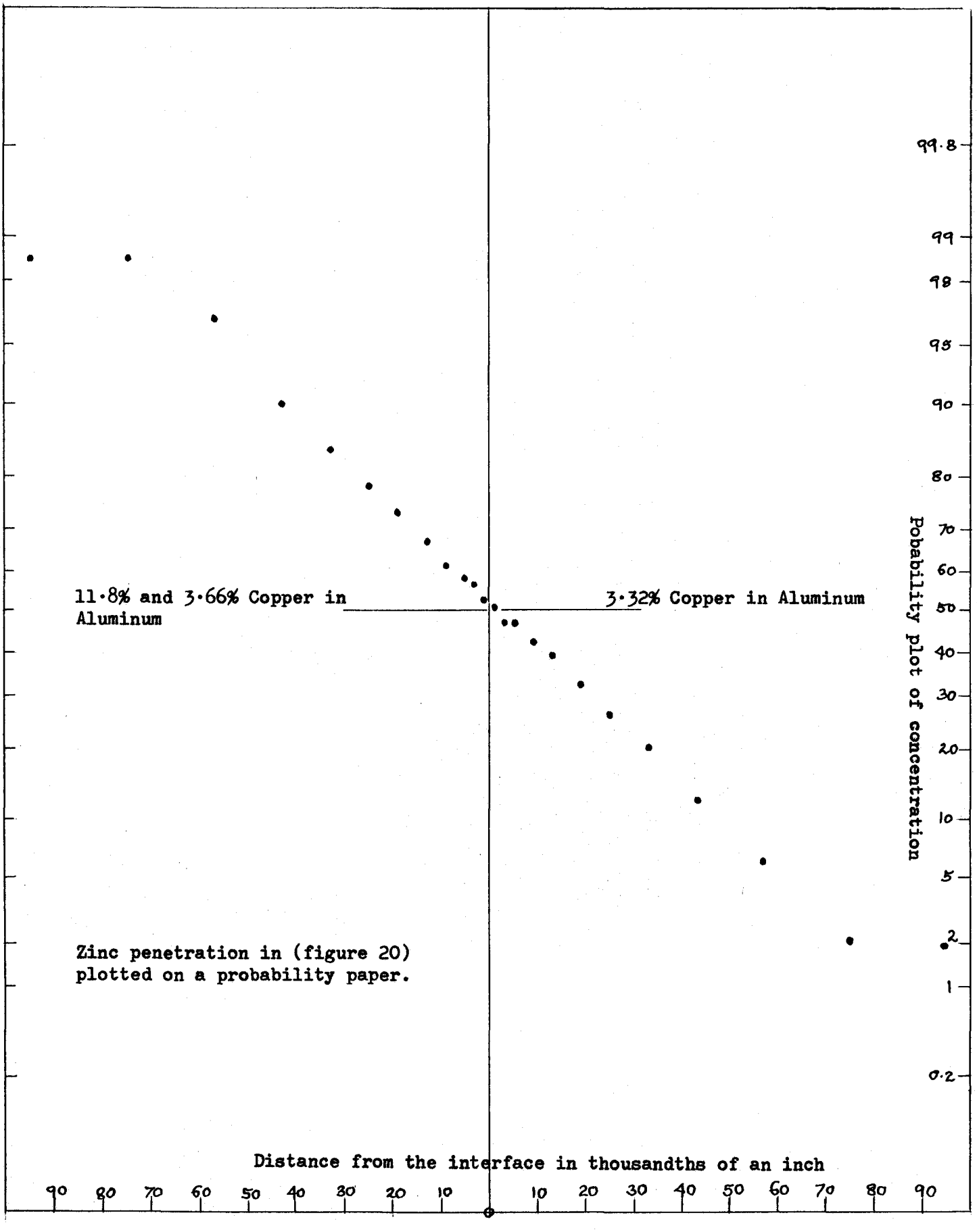
11·8% and 3·66% Copper in Aluminum
3·32% Copper in Aluminum
Zinc penetration in (figure 20) plotted on a probability paper.
Probability plot of concentration
99·8
99
98
95
90
80
70
60
50
40
30
20
10
5
2
1
0·2
Distance from the interface in thousandths of an inch
90 80 70 60 50 40 30 20 10
10 20 30 40 50 60 70 80 90

Figure 21

been corrected for proper units.

The effect of zinc gradient on copper diffusion is illustrated in figure 22. The couple used was 3·66 percent copper and 11·8 percent zinc in aluminum versus 3·32 percent copper in aluminum. The curve according to equation (57) for $D_{22} = 4{\cdot}54 \times 10^{-10}$ cm^2/second, $D_{11} = 3{\cdot}4 \times 10^{-9}$ cm^2/second and calculated $D_{21} = 9{\cdot}66 \times 10^{-11}$ cm^2/second has been traced on over the readings in figure 22. The actual value of D_{21} seems to be much lesser than the calculated value. This is because the equation (50) has been unwisely used in evaluating D_{21}. The formula is true only for $X_1 \ll X_3$ and $X_2 \ll X_3$. In the present case X_1 is quite large.

The thermodynamical interaction parameter, c, has been evaluated from the ratio (50)

$$\frac{D_{12}}{D_{11}} \simeq (1 + c)X_1 \text{ , where } X_1$$

is the mole-fraction of component 1 at the interface of the couple in figure 19. The calculated value for $c \simeq 7{\cdot}4$, based on concentration units of moles per unit volume.

For the convenience of the reader, all the D values within experimental errors, have been presented in a tabulated form in Table 2. The diffusion coefficients determined by fitting best tangents to the experimental points are also included in the same table.

TABLE 2

Specifications of couples	D	Diffusion Coefficients calculated within experimental errors in cm^2/second	Diffusion Coefficients determined by fitting best tangents to the experimental points in cm^2 /second
3·32% Cu in Aluminum vs. Pure Aluminum (Figure 13)	D_{22} (D_{Cu-Cu})	$(4·59 \pm 1·07) \times 10^{-10}$	$4·45 \times 10^{-10}$
12·6% Zn in Aluminum vs. Pure Aluminum (Figure 14)	D_{11} (D_{Zn-Zn})	$(2·915 \pm 0·265) \times 10^{-9}$	$2·905 \times 10^{-9}$
3·66% Cu and 11·8% Zn in Aluminum vs. 12·6% Zn in Aluminum (Figure 17)	D_{22} (D_{Cu-Cu})	$(1·237 \pm 0·178) \times 10^{-9}$	$1·232 \times 10^{-9}$
3·66% Cu and 11·8% Zn in Aluminum vs. 12·6% Zn in Aluminum (Figure 19)	D_{12} (D_{Zn-Cu})	$(1·61 \pm 0·15) \times 10^{-9}$	$1·65 \times 10^{-9}$
3·66% Cu and 11·8% Zn in Aluminum vs. 3·32% Cu in Aluminum (Figure 20)	D_{11} (D_{Zn-Zn})	$(3·41 \pm 0·43) \times 10^{-9}$	$3·40 \times 10^{-9}$

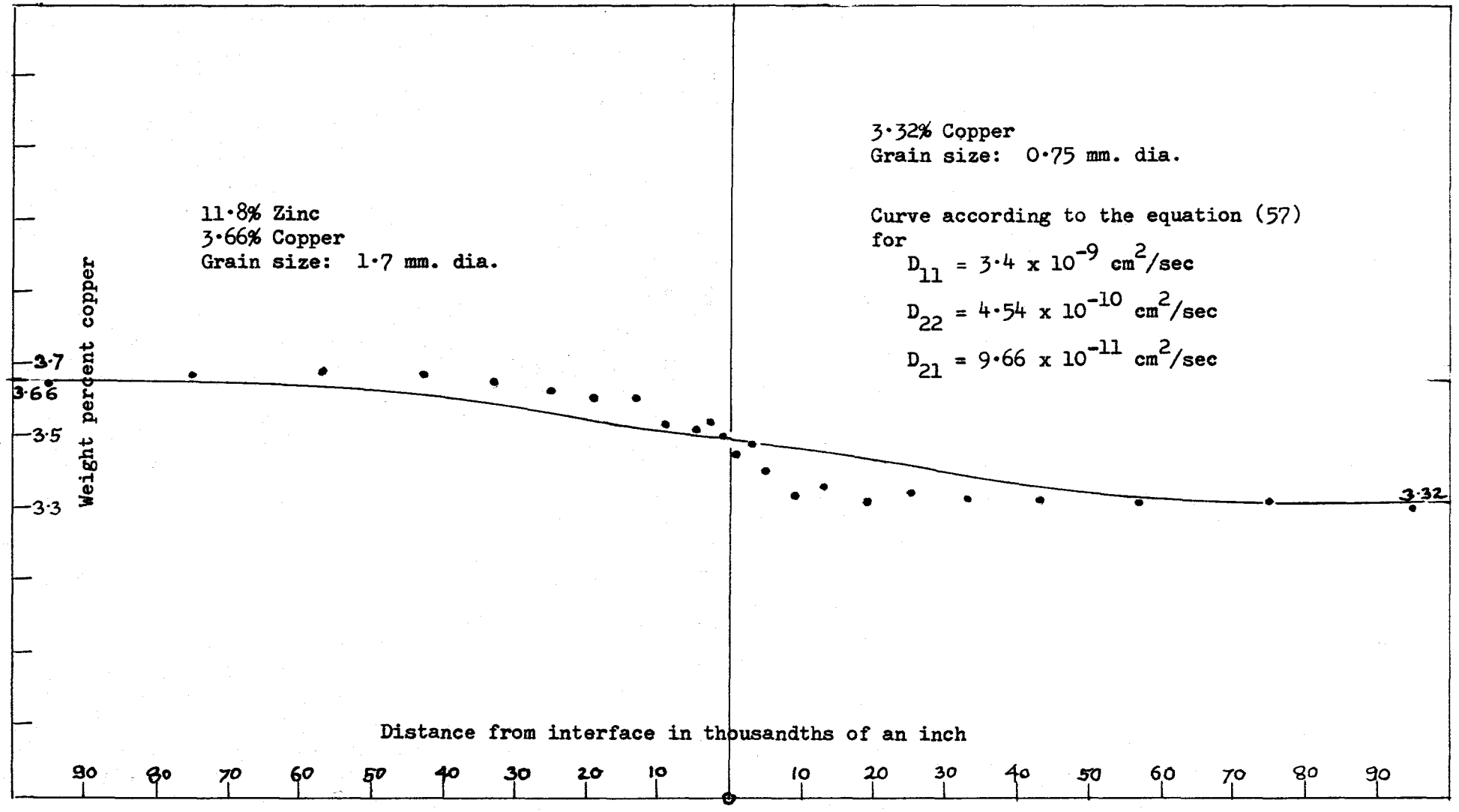

Figure 22. Effect of zinc gradient on copper diffusion.

DISCUSSION

The techniques employed were designed to minimize the effects of impurities and ingot segregation on diffusion parameters. The stock metals were of high purity (99·99), the alloys were homogenized prior to the diffusion anneal, the couples were cut from the more homogeneous sections of the rolled ingots (figure 23) and the standards were collected from the semi-infinite zones of the couples. The standards for each couple were standardized against pure metals. All the weighings were performed in a microgramatic balance. The zinc analyses were performed without any background from copper activity after allowing the copper isotope to decay. The counting error was usually kept to a maximum of 1 percent by setting the preset at 10^4. Aluminum, because of its short half-life, did not interfere with the measurements.

It was demonstrated in this investigation that zinc prefers to diffuse down the copper gradient (figure 19). In other words, copper raises the activity of zinc. This implies that zinc will raise the activity of copper since the cross-effects bear the same sign according to relation (50). Furthermore, if this be the case, the presence of zinc in duralumin should decrease the rate of precipitation of $CuAl_2$.

This conclusion follows because, when $CuAl_2$ precipitates, it grows with a corresponding depletion of copper from the surrounding

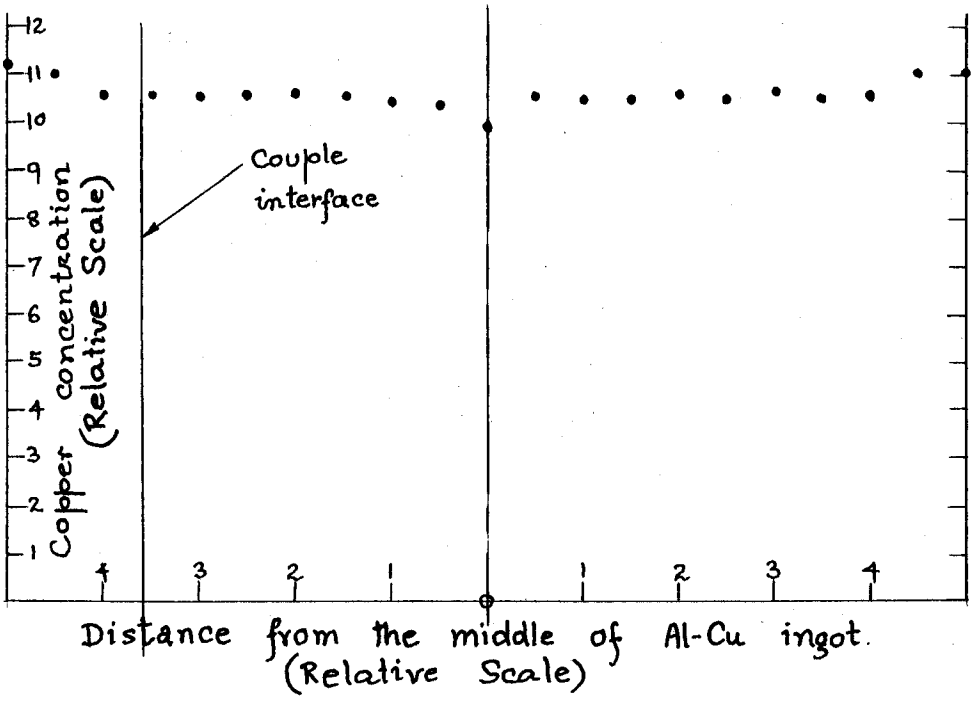

Figure 23

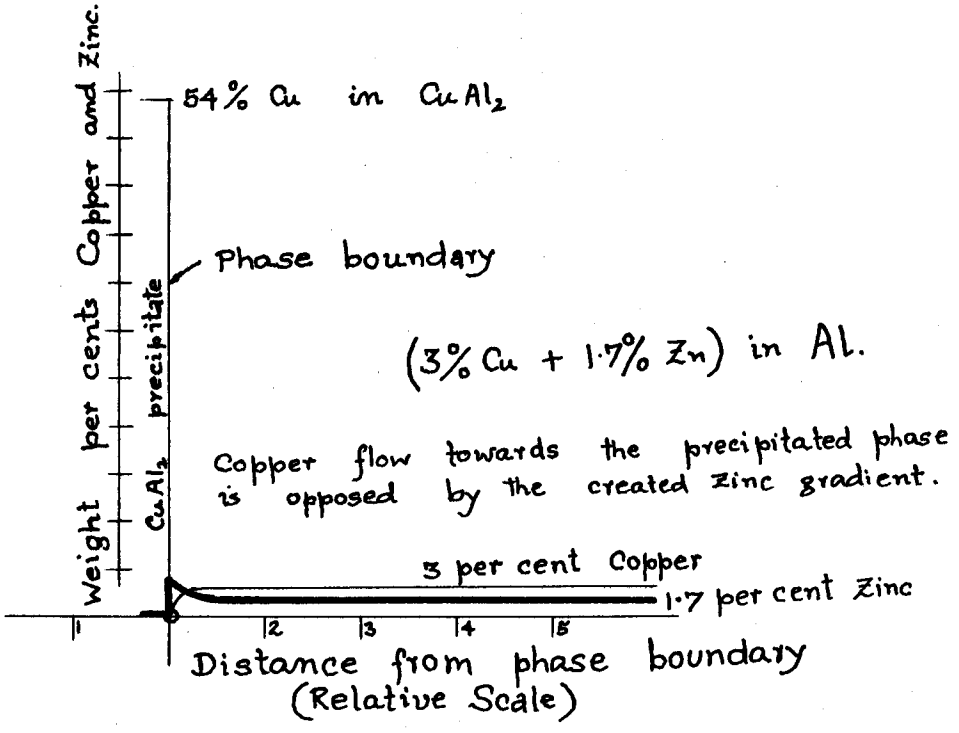

Figure 24

alloy and concurrently the zinc concentration increases in front of the precipitate boundary (the maximum solubility of zinc in $CuAl_2$ in only 1 percent at 460°C as can be seen in figure 10 and the zinc solubility in $CuAl_2$ for any specific zinc concentration in Al-Zn-Cu alloy at this temperature can be estimated by drawing approximate tie-lines from the α phase to the θ phase). This concentration gradient in front of the phase boundary opposes the copper diffusion towards the precipitate and hence the rate of precipitation of $CuAl_2$ is slowed down. In agreement with this hypothesis, it is experimentally observed that the addition of zinc to duralumin alloys decreases the precipitation rate of $CuAl_2$. To clarify these statements, the copper and zinc diffusion gradients are schematically shown in figure 24 for a duralumin alloy.

Another important conclusion, formulated from the observations of this investigation, was that when two solutes have similar diffusion coefficients, the cross-effects seem to be moderated by one another in a substitutional solution. This behavior makes the determination of cross-effects very difficult experimentally. The effect of diffusion interaction (as measured by D_{12}, D_{21}), therefore, is not a very important factor to be considered for most metallurgical purposes where diffusion zones are semi infinite in nature. The effect becomes important only when there exist some constraints present in a system. The familiar examples of such constraint are fixed boundary conditions in a steady state, finite diffusion couple, phase boundaries etc.

CONCLUSIONS

(i) The diffusion coefficients of copper and zinc at 503·6°C are 4·45 x 10^{-10} cm^2/second and 2·905 x 10^{-9} cm^2/second respectively.

(ii) The off-diagonal coefficient for the effect of copper gradient on zinc diffusion is 1·65 x 10^{-9} cm^2/second.

(iii) Zinc in a solution of copper in aluminum will lower the rate of precipitation of $CuAl_2$.

(iv) Solutes with close values of their diffusion coefficients try to moderate the effect of one another in a substitutional solid solution.

BIBLIOGRAPHY

1. Barrer, R. M. 1951. Diffusion in and through Solids (Cambridge University Press).

2. Boltzmann, L. 1894, Ann. Physik, Leipzig, 53, 959.

3. Callen, H. B. 1959. Thermodynamics (John Wiley, New York).

4. Darken, L. S. 1951. Atom Movements (American Society for Metals), p.17.

5. De Groot, S. R. 1952. Thermodynamics of Irreversible Processes (Interscience, New York).

6. Fick, A. 1855. Pogg. Ann. 94, 59.

7. General Electric Company. 1956 chart of the Nuclides (Knolls Atomic Laboratory, U. S. A. E. C.).

8. Gosting, L. J. and Fujital, H. 1956. J. Am. Chem. Soc. 78, 1099.

9. Hooyman, G. J. 1956. Physica 22, 751.

10. Kirkaldy, J. S. 1957. Can. J. Phys. 35, 435.

11. Kirkaldy, J. S. 1958. Can. J. Phys. 36, 899.

12. Kirkaldy, J. S. and Purdy, G. R. 1962. Can. J. Phys. 40, 202.

13. Mason, G. R. 1959. M. Eng. (Metallurgy) Thesis (McMaster University, Canada).

14. Matano, C. 1933. Japan J. Phys. 8, 109.

15. Onsager, L. 1945-46. Ann. N. Y. Acad. Sci. 46, 241.

16. Onsager, L. and Fuoss, R. M. 1932. J. Phys. Chem. 36, 2689.

17. Peirce, B. O. and Foster, R. M. 1956. Short Table of Integrals (Ginn and Company, Boston).

18. Prigogine, I. and Defay, R. 1954. Chemical Thermodynamics (Longman Green and Co., London).

19. Smithels, C. J. 1955. Metals Reference Book, Vol.1 (Butterworth Scientific Publications, London).

20. Smithels, C. J. 1955. Metals Reference Book, Vol.2 (Butterworth Scientific Publications, London).

APPENDIX A

Compatible to the boundary conditions (8), the solution to the equation (7) is

$$(9a) \qquad C = C^o + \frac{1}{2}(C' - C^o)\left(1 - \frac{2}{\sqrt{\pi}}\int_o^{\frac{x}{2\sqrt{Dt}}} e^{-\xi^2}\, d\xi\right)$$

Differentiating

$$(1A) \qquad \frac{dC}{dx} = -\frac{1}{2}(C' - C^o)\,\frac{2}{\sqrt{\pi}}\,\frac{d}{dx}\int_o^{\frac{x}{2\sqrt{Dt}}} e^{-\xi^2}\, d\xi$$

choosing the origin at the point, which has the corresponding concentration value equal to $\frac{1}{2}(C' + C^o)$,

$$(2A) \qquad \left.\frac{dC}{dx}\right|_{n=0} = -\frac{1}{2}(C' - C^o)\cdot\frac{2}{\sqrt{\pi}}\cdot\frac{1}{2\sqrt{Dt}}\cdot 1$$

$$(3A) \qquad = -\frac{1}{2d}(C' - C^o)$$

where d is the distance between the origin on the line passing through C^o parallel to x axis and the point of intersection of the tangent (at $C = \frac{1}{2}(C' + C^o)$ to the penetration curve with the same line.

Equating (2A) and (3A),

$$\frac{1}{d} = \frac{1}{\sqrt{\pi}\sqrt{Dt}}$$

or

$$(4A) \qquad D = \frac{d^2}{\pi t}$$